

# **RADIOTRACER TECHNIQUES FOR STUDIES OF THE LOADING PHENOMENON IN GRINDING**

A Thesis Submitted  
In Partial Fulfilment of the Requirements  
for the Degree of  
**MASTER OF TECHNOLOGY**

10172

By  
**AJIT G. GOHAD**

to the  
**NUCLEAR ENGINEERING AND TECHNOLOGY PROGRAMME  
INDIAN INSTITUTE OF TECHNOLOGY, KANPUR  
SEPTEMBER, 1976**

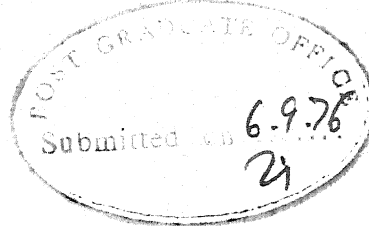
THE LOADING PHENOMENON IN GRINDING  
CONTACTER TECHNIQUES FOR STUDIES

U. T. MANOUR  
CENTRAL LIBRARY  
Acc. No. **A 47194**

14 OCT 1976

NETP-1976-M-GOH-RAD





ii

# CERTIFICATE

Certified that the present work entitled 'Radiotracer Techniques for Studies of the Loading Phenomenon in Grinding', has been carried out by Mr. A.G. Gohad, under my supervision and has not been submitted elsewhere for the award of a degree.

*Rakesh Chawla*

( R. Chawla )

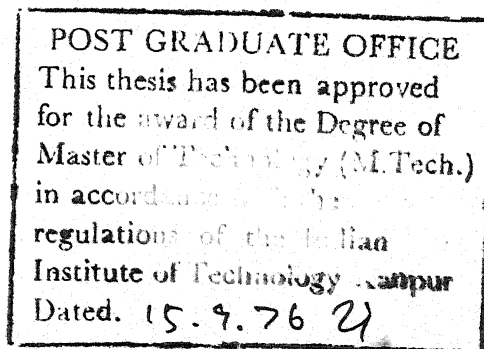
Assistant Professor

Nuclear Engineering and Technology Program

Indian Institute of Technology

Kanpur

September, 1976



## ACKNOWLEDGEMENTS

I take this opportunity to express my deep sense of gratitude and sincere thanks to Dr. R. Chawla for his inspiring guidance, invaluable suggestions and constant encouragement throughout the phase of this work. Also, my sincere thanks are due to Dr. G.K. Lal for his valuable suggestions and comments which clarified a number of points. I wish to express my sincere appreciation of the assistance I obtained from Mr. Pathak, Mr. M.M. Singh, Mr. Sarkar, Mr. Bajaj, Mr. Arora and Mr. Joginder Singh. Messrs. Misra, Tripathi and Buddhi Ram deserve my gratitude for an excellent piece of typing and cyclostyling.

It is indeed my great pleasure to express my thanks to all my friends, for their useful suggestions and cooperation in sorting out many problems.

Financial assistance is gratefully acknowledged from the Department of Atomic Energy, Govt. of India, under whose sponsorship this work was carried out.

A.G. Gohad

## CONTENTS

<u>Chapter</u>		<u>Page</u>
I	INTRODUCTION	1
	1.1 Grinding Wheel Loading	2
	1.2 The Present Work	3
II	GENERAL REVIEW	6
	2.1 The Grinding Process	6
	2.1.1 Grinding Wheels	7
	2.1.2 Grinding Operations and Performance	9
	2.2 Grinding Wheel Loading and Difficulties in its Measurement	11
	2.3 Earlier Radiotracer Applications in Metal-Cutting	14
	2.4 Health Physics Considerations	17
III	MEASUREMENT TECHNIQUES	21
	3.1 $\gamma$ - $\gamma$ Coincidence Technique	22
	3.2 Extrapolation Method	26
	3.3 Checking of Normalization Techniques	28
	3.3.1 $\gamma$ - $\gamma$ Coincidence Counting of Dressed Debris	28
	3.3.2 Conventional Measurements	30
IV	EXPERIMENTAL PARTICULARS	32
	4.1 The Grinding Machine	32
	4.2 Measurement of Forces	34
	4.3 Design of Debris-Collection Box	35
	4.4 The Counting Set-up	36
	4.5 Activation of Steel Workpieces	39
	4.6 Activation of Aluminium Samples	41
	4.7 Radiological Considerations	43

<u>Chapter</u>		<u>Page</u>
V	EXPERIMENTS, RESULTS AND THEIR INTERPRETA- TION	45
	5.1 Procedure for Obtaining Relative Loading Curves	45
	5.2 The Various Experiments with Annealed HSS	48
	5.3 Normalisation to Absolute Results	49
	5.4 Comparison of Normalisation Techniques	51
	5.5 Comparisons Between Radiotracer and Conventional Measurements	53
	5.6 Repeatability of Results	54
	5.7 Interpretation of the Loading Data Obtained	54
	5.8 Loading Measurements with Aluminium	57
VI	CONCLUSIONS AND SCOPE FOR FURTHER WORK	59
	6.1 Conclusions	59
	6.2 Scope for Further Work	62
	REFERENCES	64

## LIST OF TABLES

<u>Table</u>		<u>Page</u>
4.1	Intercalibration of the Three Different Work-piece Samples	40
5.1	Wheel and Workpiece Specifications	45
5.2	Dressing Sequence Employed	46
5.3	Grinding Conditions for the Various Experiments with Annealed HSS	48
5.4	Comparison of Normalization Techniques	52
5.5	Comparison of Conventional and Radiotracer Measurements	53

## LIST OF FIGURES

Figure

- 2.1 Variables in Surface Grinding.
- 2.2 Loading Curves from Reference No. (a) 4, (b) 5, (c) 6, (d) 7.
- 3.1 Block Diagram of  $\gamma$ - $\gamma$  Coincidence Counting Set-up.
- 4.1 Extended Octagonal Ring Type Dynamometer,  
(a) Wiring Diagram for Vertical Force,  
(b) Wiring Diagram for Horizontal Force.
- 4.2 Comparison of NaI Spectrum of Standard Co-60 Source and Irradiated Annealed HSS Piece.
- 4.3 Ge(Li) Spectra of Irradiated Steel Samples  
(a) 2 weeks, (b) 4½ months After Irradiation.
- 4.4 Neutron cross-section for Al-27 ( $n, \alpha$ ) Na - 24 Reaction [Ref. No.16].
- 4.5 NaI Spectrum of Activated Aluminium.
- 5.1 Loading Curve for Experiment No. 1.
- 5.2 Loading Curve for Experiment Nos. 2,3, and 4.
- 5.3 Loading Curve for Experiment No. 5.
- 5.4 Loading Curve for Experiment No. 6.
- 5.5 Loading Curve for Experiment No. 7.
- 5.6 Loading Curve for Experiment No. 8.
- 5.7 Loading Curve for Experiment No. 9.
- 5.8 Loading Curve for Experiment No. 10.
- 5.9 Extrapolation Curve for Experiment No. 4.

Figure

- 5.10 Relationship Between Volume of Material Removed and No. of Passes.
- 5.11 Variation of  $V_{155}$  with (a) Depth of Cut,  $d$  and (b) Table Speed,  $v$ .
- 5.12 Variation of  $V_{155}$  with Material Removal Rate.
- 5.13 Variation of  $V_{155}$  with Chip Thickness.
- 5.14 Variation of Slope,  $a$ , with Depth of cut and Table Speed.
- 5.15 Variation of Slope,  $a$ , with Material Removal Rate.
- 5.16 Variation of Slope,  $a$ , with Chip Thickness.
- 5.17 Loading Curve for Aluminium Workpiece.

Plates

- 1. General View of the Grinding Set-up.
- 2. The View of the Debris Collection Box.
- 3.  $\gamma$ - $\gamma$  Counting Set-up.

## ABSTRACT

The loading phenomenon in grinding wheels is difficult to study experimentally by conventional means. Radiotracer techniques using activated workpieces of steel (annealed HSS) and aluminium have been applied for the first time to quantitative measurements of the effects of grinding parameters on wheel loading.

For annealed HSS, the tracers employed were Co-60 and Fe-59. The amount of loaded material was determined absolutely by applying (a) a  $\gamma$ - $\gamma$  coincidence technique for counting the Co-60 activity on the cutting surface of the wheel, (b) an extrapolation method applied to singles  $\gamma$ -counting of the Fe-59/Co-60 activity on the wheel. As a check on the above techniques, absolute results for the amount of loaded material were derived by  $\gamma$ - $\gamma$  coincidence counting of Co-60 activity in dressed material collected from the wheel after an experiment. A few conventional measurements of loading involving chemical separation of metal and a use of a micro-balance were also conducted to confirm the validity of the nuclear techniques. Studies of the loading phenomenon for annealed HSS were conducted over a range of grinding conditions.



The feasibility of carrying out loading studies in the grinding of other materials of interest was established in the case of aluminium, where the  $\gamma$ -emitting radio-tracer employed was Na-24 generated from the Al-27 (n,  $\alpha$ ) reaction with fast neutrons.

## CHAPTER I

### INTRODUCTION

Improvements in the quality of the final product and higher economic efficiency are characteristic aims of modern manufacturing. The need to produce interchangeable units, as well as the aim to minimise the fitting time, has led to the requirement of more stringent tolerances on the size and shape of machined products. The role of grinding as an effective machining operation has therefore considerably increased in importance.

The grinding process, as it becomes more highly developed, holds the promise of reduced costs and higher efficiency. As castings and forgings are held to a closer stock allowance, it becomes more economical to use grinding as a stock-removal as well as a finishing process. As difficult-to-machine materials are introduced, grinding again proves advantageous. In order to realize the full potential of the grinding process, it is necessary to optimise various grinding variables such as wheel wear, surface finish and wheel loading. An important aspect is thus the development of techniques for the accurate measurement of these variables. The application of radiotracer methods to the determination of grinding wheel loading, a

phenomenon difficult to study experimentally by conventional means, is the subject of the present work.

### 1.1 Grinding Wheel Loading:

In grinding, the efficiency of the operation decreases as the wheel's cutting surface becomes dull. This dulling is due to either the abrasive points wearing down excessively to 'flats' (in which condition they do not remove metal readily), or to the loading of extraneous material into the porous surface of the grinding wheel. The loading of grinding wheels can be of two types, viz. (a) gum loading and (b) metallic loading. The former occurs when the grinding fluid used deposits a gummy material on the surface of the grinding wheel. Metallic loading is due to metal particles from the workpiece adhering to the abrasive grains and filling the pores on the wheel surface, thereby leaving insufficient room for chip clearance.

In grinding, increased loading generally brings about several undesirable effects, such as reduction in stock-removal rate and increase of instability due to chatter vibration. Further, loading causes excessive heating of the work surface due to high friction between the work and loaded material, resulting in deterioration of both surface finish and mechanical properties of the surface layer of the work. Since the loading phenomenon is not well understood, any corrective measures that are applied have to be empirical ones.

In evaluating the efficiency of a grinding operation, a determination of the power consumption is usually made. While this is an important measurement, it includes the effects of both the wearing of the abrasive grains and of metallic loading. Accordingly, separate measurements are essential to differentiate between these two contributing factors. Little attention, however, has been paid to the loading process and the means of combating it. This has been largely due to difficulties in carrying out accurate measurements of loading. A few techniques have been tried, e.g. the chemical detection method, the colorimetric method and the spectrophotometric method. Recently, two other techniques - one involving the measurement of induced currents and the other using the magnetic properties of the loaded material have been suggested for the in-process determination of loading characteristics of grinding wheels.

Some of the above methods for measuring loading have to be carried out rather painstakingly while others provide difficulties in normalization, i.e. in obtaining accurate absolute results for the amount of loaded material.

## 1.2 The Present Work:

In the present study, radiotracer techniques have been applied for the first time to experimental studies of the loading phenomenon in grinding. The radiotracers used were

Co-60 and Fe-59 for annealed HSS workpieces and Na-24 for aluminium. The amount of loaded material for the annealed HSS experiments was determined absolutely by applying a  $\gamma$ - $\gamma$  coincidence technique for counting the Co-60 activity on the cutting surface of the wheel. The basic counting method had been established earlier in absolute measurements of the wear of irradiated HSS turning tools and in the development of short-tool life testing methods. The other method used to obtain absolute results was an extrapolation method applied to singles  $\gamma$ -counting of activity on the wheel. As a check on the above two techniques, absolute results for the amount of loaded material were derived, for annealed HSS, by  $\gamma$ - $\gamma$  coincidence counting of the Co-60 activity in dressed material collected from the wheel after an experiment. A few conventional measurements of loading, involving chemical separation of metal and the use of a micro-balance, were also conducted to confirm the validity of the nuclear techniques.

Applying the above methods, the growth of loaded material on the wheel surface was studied under various dry, plunge grinding conditions. It was found that the loading curve for the annealed HSS experiments could be divided into two stages - one in which loading increases rapidly, and the other in which it remains nearly constant. The latter was considered to represent a state of equilibrium for loading

during the grinding operation. The variation of characteristic loading parameters was studied for different depths of cut and table speeds.

The feasibility of carrying out loading studies for other materials of interest was established in the case of aluminium, for which Na-24 ( $T_{\frac{1}{2}} = 15$  hours) was used as the  $\gamma$ -emitting radiotracer. This was generated employing the  $Al^{27} (n, \alpha)$  reaction with 14 MeV neutrons obtained using the Van de Graaf generator at IIT Kanpur.

## CHAPTER II

### GENERAL REVIEW

#### 2.1 The Grinding Process [1]

Over the years, the grinding process has commanded a position of ever-increasing importance in industry, so that today it is one of the most widely employed metal cutting operations. At the beginning, grinding was a method of finishing hard surfaces. Today, it is also used for the removal of large quantities of various types of materials. Although it is one of the most precise and technically important material removal operations, grinding is probably the most complex and difficult to understand.

In grinding, metal is removed by a shearing process just as in turning and milling operations. Grinding may be described as a multi-tooth operation in which a large number of abrasive grains held by a bonding material perform the cutting.

There are, however, certain important differences between the grinding process and other methods of metal removal. In grinding, the grains which act as tools are of varied and indeterminate geometry. Further, grinding is ordinarily carried out at surface speeds of 200 m/min. or

higher, while other metal-cutting operations are accomplished at speeds an order of magnitude lower. Grinding is also characterized by very small depths of cut, of the order of a few microns. Because of the random grain geometry, the high cutting speed and the small depth of cut, the mechanisms involved in grinding are difficult to observe and evaluate.

### 2.1.1 Grinding Wheels:

A grinding wheel is composed of a large number of small abrasive particles held together by a bonding agent. These abrasives are extremely hard ( $\sim 2000 \text{ kgf/mm}^2$ ), brittle and refractory particles. Typical abrasives used are (i) Aluminium Oxide (alundum) denoted by the letter 'A', (ii) Silicon Carbide (Carborundum) - 'C', and (iii) Diamond - 'D'. Silicon carbide is more suitable for grinding materials of low tensile strength, while alumina is most efficient for grinding hard and tough materials.

The structure of the grinding wheel is characterized by:

(a) the mean force required to dislodge a grain from the surface of the wheel. This is called the grade of the wheel, designated by a letter of the alphabet. The wheel grades are: C to G (very soft), H to K (soft), L to O (medium), P to S (hard) and T to Z (very hard).



(b) the mean void size and distribution. This is designated by the structure number which varies from 1 to 12, where 1 represents a very dense structure and 12 a very open one.

(c) the mean spacing of active grains on the wheel surface. This depends on the grain size, the amount of bonding material, the dressing technique and the grain type. The range of grain sizes is: 6 to 24 (coarse), 30 to 60 (medium), and 70 to 600 (fine).

There are six general types of bonds used in grinding wheel manufacture: (i) Vitreous (V), which consists of a glassy, brittle, high-strength material such as pyrex glass, (over 75 percent of all grinding wheels have this type of bond), (ii) Resinoid (B), which consists of organic thermosetting resins, (iii) Rubber (R), (iv) Silicate (S), (v) Shellac (E), (vi) Magnesite (O) and (vii) Metallic (M).

Using the above notations, a typical grinding wheel may be designated as follows:

A	46	H	8	V	BE
Abrasive	Grain	Grade	Structure	Vitrified	BE Type
Aluminum	Size 46	H	Number 8	Bond	Vitrified
Oxide					Bond

Grinding wheels are 'dressed' by machining the wheel surface by a diamond tool. This produces a round wheel and removes flats from worn grains by grain fracture or removal. The manner in which a wheel is dressed can have a significant effect on its grinding performance. Therefore, for experimental work, one must hold the down feed, cross-feed rate, etc. constant during dressing, in order to reproduce wheel conditions.

A grinding wheel is 'trued' in order to restore its cutting face to running truth or to alter the cutting face for grinding special contours.

#### 2.1.2 Grinding Operations and Performance:

Four main types of grinding operations are generally employed, depending on the job to be manufactured.

- (i) Surface Grinding: grinding a plane surface.
- (ii) Cylindrical Grinding: Grinding a cylindrical surface.

It can be subdivided into (a) External and (b) Internal.

- (iii) Centreless Grinding: Grinding the inside or outside diameter of a cylindrical workpiece not mounted on centres.
- (iv) Off-hand Grinding: when the dimensional accuracy is unimportant.

When the material to be ground is narrower than the width of the wheel, the operation is called Plunge Grinding.

For the case of surface grinding, Fig. 2.1 indicates the important grinding variables - wheel speed ( $V$ ), table speed ( $v$ ), down feed or depth of cut ( $d$ ), wheel diameter ( $D$ ), and undeformed chip thickness ( $t$ ). The other variables are the number of cutting points per unit length of wheel surface ( $C$ ) and the width-to-depth ratio of an average cut ( $r$ ).

The performance of a grinding wheel can be assessed in terms of 'grindability', a term used to describe the relative ease of grinding. Grindability is concerned with the forces, power required in grinding, wheel wear and stock-removal rate, as well as the surface finish produced. A material is said to have good grindability if the forces, power and wheel wear are low, the stock-removal rate is high and the surface finish is good. Most of the factors affecting grindability can be shown to be related to the undeformed chip thickness given by the equation [2]

$$t = \sqrt[3]{(4v/VCr)\sqrt{(d/D)}}$$

The ease of grinding is mainly assessed in terms of the following three indices:

- (1) Volume ratio or Grinding ratio =  $\frac{\text{Volume of metal removed}}{\text{Volume of wheel worn}}$
- (2) Grinding characteristic =  $\frac{\text{Grinding ratio}}{\text{Net horse-power}}$
- (3) Grinding Rating =  $\frac{\text{Grinding ratio}}{(\text{Power per unit volume removal rate}) \times \text{Surface finish (RMS)}}$

For good grinding conditions, the above three indices should be as large as possible. A grinding fluid is sometimes used to improve the cutting conditions as well as surface finish.

## 2.2 Grinding Wheel Loading and Difficulties in its Measurement:

The loading of work material into the pores of a grinding wheel is one of the main factors which directly affects grinding performance. Loading gives rise to several detrimental effects such as excessive vibrations, reduced material removal rate, excessive grinding temperatures resulting in thermal cracks and metallurgical changes at the work surface, etc. In practice, it is necessary to dress the wheel when the loaded amount reaches a certain critical value which causes serious reduction in cutting efficiency.

Because of difficulties encountered in carrying out measurements of loading, only a few systematic investigations of the phenomenon are presently found in the literature. A review of experimental techniques used to date is given below:

(1) Shudolz et al [3] suggested the 'transfer' or 'chemical detection' method in which metallic loading images from the wheel surface, where maximum loading was observed, were recorded on HCl treated paper. The wheel loading impressions were then counted accurately and the degree of wheel loading was determined by measuring the number of

particles per unit area at two different positions, where maximum loading was apparent. The average number of particles determined from these impressions gave the maximum degree of loading.

(2) Khudobin [4] developed a colorimetric method to determine the degree of wheel loading. Samples of loaded material were taken from five different points on the wheel surface, brought into solution and then treated with a reagent (Ammonium Thyocyanate) to impart a stable orange colour to the solution indicating the presence of iron. A measure of the concentration of iron in the solution was obtained by using a KM colorimeter. The amount of iron loaded on the wheel surface could then be deduced by comparing the samples with standard solutions. It was observed that loading increases with grinding time in the manner indicated in Fig. 2.2(a).

(3) The method of Pandey et al. [5] involves obtaining scratched samples of similar weight from the wheel surface, chemically separating the loaded metal from the abrasive grains and determining the transmittance of the resulting solution using a spectrophotometer. Calibration was again carried out using standard solutions. The experimental results indicated that a newly dressed wheel would tend to load very rapidly in the beginning but that, after the initial period,

loading proceeds more or less at a constant rate [Fig.2.2(b)]. It was also observed that loading increases with increasing down feed and table speed, that large grain-sized wheels are less susceptible to loading, and that wheels which wear rapidly would load to a lesser extent than wheels which do not.

(4) Recently, an eddy current sensor for inprocess measurement of loading has been developed by Sata et al.[6]. The sensor is based on the inductive effect between a coil placed closed to the wheel surface and the loaded metal particles on the wheel surface. With a d.c. current flowing in the coil, a slight change of the voltage is caused by the loaded particles. The voltage is amplified and, by rectifying the output of the amplifier, the mean coverage of the loaded metal on the wheel surface can be obtained. Calibration was carried out through subsidiary experiments using plastic wheels embedded with sliced steel wires of various diameters. Sata, et al., have reported that loading increases gradually with grinding time and that a higher metal removal rate in grinding gives a higher loading rate [Fig. 2.2(c)].

(5) In the work of Yamamoto and Maeda [7], a method for in-process measurement of loading has been developed on the basis of magnetic properties of the loaded material. A d.c. magnetizing method based on the principle of magnetic recording/reproduction was employed. The variation of loading with grinding

time was evaluated and found to be of the type indicated in Fig. 2.2(d).

In the above methods, the following difficulties in the experimental techniques may be identified:

- (i) The need for painstaking sample preparation involving chemical separation, etc., in (2) and (3).
- (ii) The sampling of only a small part of the loaded wheel surface, in (1), (2) and (3).
- (iii) Difficulties in obtaining accurate absolute results in (4) and (5).

The presently developed radiotracer methods do not have any of these drawbacks.

### 2.3 Earlier Radiotracer Applications in Metal-Cutting:

Normal tool-life testing takes a lot of time, so that accelerated tests are often applied. These tests, however, cannot be accelerated beyond a certain limit due to the intrinsic low sensitivity of conventional wear measuring techniques. The use of radioactive tools for measuring wear, on the other hand, provides sufficiently high sensitivity for obtaining even the instantaneous rates of tool wear at any given time in the life of a tool.

During the past two decades, a number of workers have reported such measurements [8,9,10]. It has been established that 95 percent of worn particles from the cutting tool

adhere to the chips even in wet cutting. Cook and Lang [11] have pointed out some of the limitations of using radiotracer methods for tool wear determination, but the criticism has been principally of the methods employed rather than of the attainable accuracy.

Much of the earlier work employed Geiger-Muller counting of  $\beta$ - or  $\gamma$ -radiation, although NaI scintillation counters, with their high efficiency for  $\gamma$ -rays, have now become popular for such measurements. No matter which type of nuclear detector is employed, a basic problem is the accurate deduction of absolute wear from the relative counting of the chip samples. This is because of the complex counting geometry offered to the detector by a particular chip sample. Several different methods have been used for obtaining the wear absolutely, and these are listed below:

(1) In one method [9], the specific activity of the tool bits is calculated from irradiation and nuclear data. Assuming that the counting efficiency for the chip samples can be determined by subsidiary experiments, the absolute activity in a given sample can be measured and hence, the wear volume represented in it can be deduced. Such an approach obviously has serious sources of systematic error.

(2) The most commonly applied method has been to irradiate a weighed piece of tool material together with the tool bit.



This reference sample is dissolved in a suitable chemical agent, a known part of the solution is evaporated and its activity measured under identical geometrical conditions as used for measurements with chip samples [9,11]. This procedure is obviously painstaking. Besides, finite differences in simulating the chip-sample counting geometry can lead to large errors in the normalization of results.

(3) In another suggested method [10], the radiotracer is chemically separated from the weighed piece of tool material as well as from a given chip sample. The two  $\beta$  activities, in some suitable solution form, are then compared using liquid scintillation counting techniques. Here the chemistry of separating the radiotracer from the rest of the chip sample is tedious. Besides, the extreme sensitivity of liquid scintillation counting can be a major drawback.

(4) Recently, Bhattacharya [12] has reported the application of  $\gamma$ - $\gamma$  coincidence counting methods for deducing absolute total wear volumes. It has been demonstrated that consistent absolute results can be obtained irrespective of the exact counting geometry offered by a given sample of randomly rearranged chips. This method of normalization was successfully used in carrying out multispeed tool-life tests wherein, by suitable interpolation of the instantaneous rates of absolute wear measured for a number of discrete cutting speeds, the

corresponding tool-life values were deduced in a test employing a single cutting edge.

Of the methods listed above for obtaining absolute results in tool wear studies, the one which seems most suitable for applying to measurements of grinding wheel loading is (4). Using activated workpieces, one would count the loaded surface of the wheel and, in the end, normalise results by  $\gamma$ - $\gamma$  coincidence counting, i.e. without having to treat the wheel chemically and prepare special samples. However, this method would be employable only if the radio-tracer generated in the workpiece decayed through the emission of two or more coincident  $\gamma$ -rays and further, if these  $\gamma$ -rays were of sufficiently high energy for self-absorption effects in the wheel to be small. Co-60 and Na-24 are two examples of such radiotracers. In general, if the available radiotracer, say Fe-59, does not have coincident  $\gamma$ 's in its decay, an alternative approach would have to be adopted for normalization. The various normalization techniques used in the present work are described in Chapter III.

## 2.4 Health Physics Considerations:

A fundamental aspect of radio-isotope applications is the need to protect people against the harmful effects of exposure to nuclear radiation. The radiological hazards can arise either from an external source or internally through

accidental inhalation/ingestion of radioactive material. Special precautions have to be taken, therefore, for monitoring radiation levels at all stages of experimentation. Further, any radioactive waste materials generated, e.g. counted chip samples in tool-wear studies as well as the worn out radioactive tools, have to be stored and later disposed off suitably without risking any environmental contamination.

The current recommendations of the ICRP (International Committee for Radiation Protection) regarding maximum permissible levels are:

(i) For occupationally exposed individuals:

3 rems in 13 weeks, 5 rems in 1 year. A maximum continuous working exposure of 2.5 m rem/hr. An accumulated dose of  $5(N-18)$  years, where N is the age of the person.

(ii) For the General Public:

A total body exposure of less than 0.5 rem/year.

It may be mentioned at this point that the total dose accumulated during the course of the present work was less than 0.5 rem.

Four important parameters control the external radiation exposure in a given experiment, viz. (i) source strength, (ii) source distance (iii) exposure time (iv) source shielding. The dose received is directly dependent on the source strength and exposure time, and inversely on the square of

the source distance, so that experiments using radioactive materials should be so planned that minimum source strengths can be employed, personnel can be adequately distant from the source, and a minimum amount of time has to be spent in the area. If these three controlling factors are not practical, adequate shielding of the source would have to be provided.

Whenever radioactive material enters the body, it constitutes a source of internal radiation which may or may not be localized depending on the behaviour of the particular element within the biological system. A radionuclide, or a compound containing a radionuclide, on entering the body behaves exactly the same as if the corresponding stable isotope of the element were present. This means that once within the body little or nothing can be done to reduce the radiological hazard from internal sources. Consequently, the only method of achieving adequate radiation protection against internal sources lies in ensuring the prevention of the entry of radio-nuclides in quantities greater than are considered acceptable hazards.

In the present work, the workpiece itself was radioactive, whereas in tool-wear studies it is the cutting tool which is activated. However, the specific activity of the workpiece in the grinding studies was very much less than that generally used for irradiated tool bits (  $\sim 3 \mu \text{ Ci/gm}$  compared to  $\sim 3 \text{ m Ci/gm}$ ), so that source shielding was not necessary.

The complicating factor, however, was that the chips themselves were radioactive and, at the same time, of particulate size. There was thus the danger of activity being air-borne to cause equipment contamination and accidental inhalation/ingestion of radioactive dust. Special precautions had therefore to be taken, e.g. confining all the generated chips to within a double walled debris-collection box, lined on the inside with petroleum jelly (Chapter IV).

## CHAPTER III

### MEASUREMENT TECHNIQUES

As discussed in Section 2.2, some of the conventional methods employed to determine the amount of material loaded in a grinding operation are rather painstaking, involving chemical treatment of samples collected from the wheel surface. Others provide difficulties in normalization, e.g. the use of 'standard' loaded wheels for calibration. The presently developed radiotracer techniques using activated workpieces overcome these difficulties and provide a more convenient means of carrying out detailed and accurate investigations of the loading phenomenon.

Two basic methods have been presently employed for obtaining the loaded amount absolutely from observed count-rates of the wheel surface, viz.

- (i)  $\gamma$ - $\gamma$  coincidence technique for determining Co-60 activity on the cutting surface of the wheel.
- (ii) An extrapolation method, applied to singles  $\gamma$ -counting of Fe-59/Co-60 activity on the wheel surface.

As a check on these two methods, absolute results for the amount of loaded material were also derived by  $\gamma$ - $\gamma$

coincidence counting of Co-60 activity in dressed material collected from the wheel after an experiment. Further, a few conventional measurements of loading were conducted to confirm the validity of the nuclear techniques.

### 3.1 $\gamma$ - $\gamma$ Coincidence Technique:

In many practical applications of radio-isotopes, an accurate knowledge of the absolute activities of sources is unnecessary, the only requirement being relative counting of different samples of the same isotope offering the same counting geometry. However, in some applications, the activity to be counted is not of a geometry which can be easily simulated by a standard source, e.g. chip samples in tool-wear studies. This is also the case for the counting of a grinding wheel.

The coincidence method is a useful technique for eliminating geometry and efficiency considerations in the counting of samples which decay through the simultaneous emission of two or more radiations [13]. If the coincident radiations are relatively high energy  $\gamma$ -rays, so that self-absorption effects are small, the activity of distributed sources can be normalised through  $\gamma$ - $\gamma$  coincidence counting. Co-60 and Na-24 are two examples of radiotracers for which such measurements could be carried out.

The block diagram of a  $\gamma$ - $\gamma$  coincidence set-up is shown in Fig. 3.1. A point source of absolute activity  $N$ , emitting two  $\gamma$ -rays ( $\gamma_1$  and  $\gamma_2$ ) in coincidence, is located between the two  $\gamma$ -counters, A and B. If the two detectors are set such that A is sensitive only to  $\gamma_1$  and B only to  $\gamma_2$ , then the respective count-rates would be,

$$C_A = \eta_A \cdot N, \quad C_B = \eta_B \cdot N \quad (1)$$

where  $\eta_A$  and  $\eta_B$  are the overall efficiency factors for the detectors A and B and include both the geometrical as well as intrinsic efficiencies.

A coincidence is said to occur when a count is registered simultaneously in both counters, i.e. a true coincidence may be defined as one in which  $\gamma_1$  and  $\gamma_2$  are recorded simultaneously. Thus, the true coincidence rate would be

$$C_c = \eta_A \cdot \eta_B \cdot N \quad (2)$$

and hence from equations (1) and (2),

$$N = \frac{C_A \times C_B}{C_c} \quad (3)$$

The absolute activity of the radioactive sample would thus be deduced.

The true count-rates ( $C_A$ ,  $C_B$  and  $C_c$ ) have to be deduced from the measured values through the application of the following corrections:



(i) Dead-Time Corrections:

The count-rates are corrected for losses due to dead-time effects in the two counter channels. In particular, the correction factor for the recorded coincidence rate is equal to the product of the factors appropriate to the recorded rates in the two channels.

(ii) Background Corrections:

The appropriate background rates must be subtracted from the measured count rates.

(iii) Random Coincidence Rate Correction Applied to  $C_c$ :

There is, in addition to background, a contribution to the observed coincidence rate from coincidences which occur at random between unrelated counts in the two input channels of the coincidence unit. If  $m_1$  and  $m_2$  are the observed count-rates in the individual channels of the coincidence unit and if  $\tau_1$  and  $\tau_2$  are the individual resolving times of the two channels, then the random coincidence rate will be given by,

$$C_r = m_1 m_2 (\tau_1 + \tau_2)$$

The ideal conditions assumed for obtaining equation (3) are seldom achieved. It is not always possible to make a given detector sensitive to one radiation only, and corrections may have to be applied for the sensitivity of the

detector to the other radiation. Hence, one has to effectively modify equation (3) to the form,

$$N = \frac{C_A \cdot C_B}{C_C} f(\epsilon) \quad (4)$$

where  $f(\epsilon)$  is a function of the different intrinsic efficiency factors of the two detectors for the two types of radiations. It should be noted that equation (4) is independent of any geometrical efficiency factor. Thus, if sample 1 of the radioactive isotope in question offers a geometry different to that of sample 2 of the same isotope, coincidence counting would directly yield the ratio of their activities, since  $f(\epsilon)$  in equation (4) would be common to both samples.

The other effect which should be taken into account, in computing absolute activities by coincidence methods, is that of angular correlation between the coincident radiations. This is a second order effect in comparing activities of samples of the same radioisotope when the counting geometries are not very different. However, in the present study, this effect had to be considered explicitly because the geometry offered to the detectors by the wheel surface was quite different from that offered by a small reference sample.

The method outlined above was employed for deducing the absolute amount of material loaded on the wheel surface in the following way. A small, accurately weighed piece of the work

material ( $x$  gm, with  $x \approx 0.022$ ) was irradiated along with the workpiece so that the specific activity of this small reference sample would be the same as that of the workpiece. After obtaining the shape of the loading curve (relative) through singles  $\gamma$ -counting of the wheel surface,  $\gamma$ - $\gamma$  coincidence counting of Co-60 activity was used to yield  $[N_w \cdot f(\epsilon)]$  from equation (4), where  $N_w$  denotes the absolute Co-60 activity of the finally loaded amount. Coincidence counting was carried out for the small reference sample, before and after coincidence counting of the wheel. The mean count-rates from these two sets of readings for the reference sample were used in equation (4), so that the effects of electronic drift, etc. would be minimum in the result for  $[N_s \cdot f(\epsilon)]$ , where  $N_s$  denotes the absolute Co-60 activity in the reference sample. Thus, the ratio  $(N_w/N_s)$  was accurately determined and the amount of finally loaded material deduced as,

$$M_1 = [(N_w/N_s) x] \text{ gms} \quad (5)$$

### 3.2 Extrapolation Method:

Another method of normalisation based simply on singles  $\gamma$ -counting of the activity on the wheel surface was established. This method is particularly useful when the available radiotracer does not decay with the emission of two  $\gamma$ 's in coincidence, e.g. Fe-59 in mild steel.

The method involves sticking small reference samples of the irradiated work material symmetrically along the wheel's circumference, and then varying their distance from the cutting surface by using spacers of unirradiated work material. Thus, three reference pieces of similar weight, were first stuck directly on the wheel surface to form an equilateral triangle. The sum of the two detector count-rates obtained with the samples in this position was taken as the singles count-rate corresponding to a wheel/sample spacing equal to the half-thickness of the samples. A second singles count-rate was obtained with one spacer stuck between each of the reference samples and the cutting surface of the wheel. This singles count-rate corresponded to a wheel/sample spacing equal to the sample half-thickness plus one spacer thickness. The counting was repeated with two, and then three, spacers stuck between each reference sample and the wheel circumference. In this way, the dependence of the singles count-rate from the samples on the wheel/sample spacing was established.

It is easily seen that if this count rate is extrapolated to zero wheel/sample spacing, the result (say,  $C_{s0}$ ) would correspond to the singles count-rate which would be obtained if the total mass of the reference samples (say  $y$  gms), were embedded in the pores of the wheel's cutting surface. Such extrapolation would essentially take into account:

- (i) the slightly different counting geometry offered by the reference samples and
- (ii) self absorption effects in the  $\gamma$ -counting of the samples.

Thus, if at the end of a grinding experiment, the singles count-rate obtained from the wheel is  $C_w$ , the finally loaded amount would be given by

$$M_1 = \left[ \frac{C_w}{C_{so}} y \right] \text{ gms} \quad (6)$$

### 3.3 Checking of Normalization Techniques:

#### 3.3.1 $\gamma$ - $\gamma$ Coincidence Counting of Dressed Debris:

As a check on the above two methods, the amount of loaded material was also derived absolutely by  $\gamma$ - $\gamma$  coincidence counting of the Co-60 activity of dressed material collected from the wheel after an experiment.

At the end of the experiment, after coincidence counting the wheel, etc., the wheel was dressed to a depth sufficient to remove all the loaded material. The dressed debris, containing petroleum jelly and abrasive grains as well as the loaded material, was collected and packed into a pill-box. This was then coincidence counted to give the absolute amount of work material in the dressed debris, through comparison with coincidence counting results for a reference sample of work material. It is clear that the loaded amount of material thus

obtained should agree with values of  $M_1$  obtained from equations (5) and (6), i.e. from coincidence counting of the loaded wheel itself and the extrapolation method.

In the course of the experiments, it was observed that some residual activity (5-15 percent) remained on the wheel even after dressing to a depth of 100  $\mu$  (considered very much more than sufficient to remove all the loaded material). It was felt that this was due to work material sticking to the faces (non-cutting surface) of the wheel, and that this could be caused either during the grinding operation itself or during the dressing process.

In order to resolve this ambiguity, a few subsidiary experiments were carried out. After the grinding operation and before dressing the wheel, each face of the wheel was covered with two thin rubber sheets. After dressing, the top sheet from each face was removed and counted. Significant activity was observed. The wheel, now with only the bottom rubber sheets on the faces, was counted and no residual activity could be observed.

It was thus established that some work material was deposited on the faces of the wheel during dressing - and not during the grinding operation itself. Accordingly, an appropriate correction was applied in deducing  $M_1$  values from  $\gamma$ - $\gamma$  coincidence counting of the dressed debris.

### 3.3.2 Conventional Measurements:

A few conventional measurements, to determine the amount loaded on the wheel, were carried out as a check on the validity of the radiotracer techniques.

A grinding experiment was conducted with an unirradiated workpiece of exactly the same dimensions and material as the irradiated workpieces used in the radiotracer measurements. Grinding conditions were kept the same as for one of the radiotracer experiments (viz. Expt. 5, Chapter V). After five passes, the loaded amount was removed by dressing the wheel and the dressed debris was collected. The petroleum jelly in the debris was dissolved out using trichloroethylene, so that the abrasive grains and loaded material would be separated by filtering the solution. This mixture of grains and metal was weighed accurately using a Standard Analytical Balance Type SAHM 68. It was then treated with aqua-regia so as to dissolve the loaded material. The abrasive grains could then be separated and weighed accurately. The difference of the two weighings gave the mass of loaded material in the dressed debris. A correction of 10 percent was applied to this result to account for material deposited on the wheel faces during dressing (See 3.3.1).

The grinding experiment was restarted and this time stopped after 10 passes. The wheel was dressed and the amount loaded determined as earlier. Restarting each time, the loading was then measured for 15, 20 and 30 passes. The loading curve thus obtained compared reasonably well with the radiotracer technique results (Sec. 5.5).



## CHAPTER IV

### EXPERIMENTAL PARTICULARS

This chapter gives details of the various equipment employed for the experiments, the procedures adopted for activation of workpiece samples, and the health physics precautions that were observed during experimentation.

#### 4.1 The Grinding Machine:

A surface grinding machine with horizontal spindle manufactured by JAYEMS Engineering Co., Bombay, was used for the experiments. The machine was powered by a 1 HP a.c. motor. Through the use of a stepped pulley arrangement for the belt drive, grinding wheel speeds of 2000 and 3000 rpm were available. The dimensions of the grinding wheel that were constrained by the size of the mounting spindle were:

Wheel bore = 32 mm; Maximum wheel thickness = 19 mm

There was no built-in arrangement with the grinding machine for powered table movement (traverse), only a hand-wheel being provided for the purpose. However, in order to obtain different constant table speeds for the experiments, the handwheel shaft was coupled to a 0.3 HP, variable speed, GEC motor. The motor r.p.m. was measured for different positions of the speed-control lever using a tachometer. The

r.p.m. was then related to the linear speed of the table. With this arrangement, controllable table speeds in the range 0-36 m/min. were obtainable.

Depth of cut (down feed) was given by the downward vertical movement of the horizontal spindle. This was achieved by rotating a handwheel with a graduated scale. In order to calibrate this scale for the vertical movement of the spindle, some experiments were carried out in which the volume of material removed for different number of passes was measured, keeping the down feed rate constant. This measurement was carried out by noting the actual change in depth obtained with a CM-10 dial gauge indicator, mounted on a Starret's magnetic stand. Volume of material removed was then plotted against number of passes, which gave a straight line indicating the linear relationship between the two. The depth of cut  $d$ , given by

$$\begin{aligned} d &= \frac{\text{Volume of material removed}}{\text{Area of work piece} \times \text{Number of passes}} \\ &= \frac{\text{Net change in depth}}{\text{Number of passes}} \end{aligned}$$

was related to the number of divisions through which the handwheel had been rotated during each cut (pass). It was thus determined that each division on the graduated scale corresponded to a depth of cut of 13 microns (0.013 mm).

Plate 1 gives a general view of the grinding machine.

#### 4.2 Measurement of Forces:

In surface grinding, the force components of interest are  $F_n$  (normal to cutting surface) and  $F_t$  (tangential). These were measured by using an extended octagonal-ring type, two component, strain-gauge dynamometer [14], shown schematically in Fig. 4.1. In bonded-wire strain gauges [15], the basic principle is that when a wire is subjected to tension, its electrical resistance changes. If such a piece of wire is connected over a structural element under strain, the change in resistance in the wire can be used to indicate the magnitude of strain. Although, the actual change in resistance in a single active strain gauge is very small, the output can be amplified by using four active strain gauges, 1,2,3,4, in a Wheatstone bridge circuit with 1 and 4 strained in tension and 2 and 3 strained in compression.

Using a Wheatstone bridge circuit for each of the force components, as indicated in Fig. 4.1, the output voltages were amplified using strain indicators Type - 301 A and Type - 304 made by NAI Bangalore. The amplified output voltages were then fed to an Encardio-rite recorder to obtain a dynamic record of forces during each cut. The dynamometer was calibrated vertically upto 17 kgf and horizontally upto 12 kgf by using dead weights. The calibration was checked

frequently for drift. Both the vertical and horizontal responses were linear, and there was negligible interaction between the two.

#### 4.3 Design of Debris-Collection Box:

In grinding operations, unlike in other material-removal processes, the material is removed in the form of very small chips. Further, in the present work, since the workpiece was activated, the chips themselves were radioactive. Due to the particulate size of the chips, there was finite danger of activity being airborne and causing equipment contamination or accidental inhalation/ingestion of radioactive dust. Therefore, it was essential that all the chips produced be confined to within an enclosed chamber.

A suitable, double-walled perspex box was designed to enable grinding and dressing operations to be carried out within its enclosed space. It essentially consisted of two individual boxes made from 5 mm. and 10 mm perspex sheets. The inside surfaces of the boxes were smeared with a thin film of petroleum jelly before each experiment to ensure sticking of debris.

The inner box was of 300 mm x 175 mm x 60 mm. size and enclosed the grinding wheel and workpiece (or dressing tool), so that almost all the chips (or dressed debris) could be collected within it. The rear wall of the box was mounted on

the horizontal spindle casing and the other side walls could be easily screwed into position. The inner box rested on a large perspex plate which could move with the table, two vertical strips mounted on the plate remaining in sliding contact with the front and rear walls of the box. The workpiece (mounted on the dynamometer, which was in turn fixed to the table) protruded through a hole in this plate. The length of the inner box was such as to allow within it the complete longitudinal movement of the workpiece during the grinding operation. A vertical sliding arrangement was provided for the side walls of the inner box, so that down feed could be given to the grinding wheel without any interference.

The inner box was itself enclosed in an outer perspex box of 575 mm x 200 mm x 175 mm size. This was done as a precaution to ensure collection of any chips that might escape the inner box. The outer box rested inside a base tray which was fixed to the table of the grinding machine.

A view of the grinding machine with the inner and outer boxes in position is given in Plate 2.

#### 4.4 The Counting Set-up:

Singles and  $\gamma$ - $\gamma$  coincidence counting of the wheel, reference samples and pill-boxes was carried out on a twin NaI-scintillation counter system, the block diagram of which

is indicated in Fig. 3.1. The modules were of ECIL design with specifications as detailed below:

1. Scintillation Counter Heads:

SH 643, SH 644, with NaI (Tl) Crystals of 50 mm x 50 mm size, RCA 8053 photomultipliers, built-in preamplifiers, operating voltage of + 1.0 to 1.5 kV and a resolution of  $\sim 8$  percent for the Cs - 137 photopeak (0.66 MeV).

2. Amplifiers:

PA 521, settings used being 10-50 attenuation, 0.1-0.3 gain, 1  $\mu$  sec time constant.

3. Single Channel Analyzers:

SC 603 with a base line voltage range of 0.2-10 Volts and window width adjustable between 0-2 volts and SC 604 A, with a baseline voltage range of 0.2-10 Volts and window width adjustable between 0-1 Volt.

4. High Voltage Units:

HV-216, with positive output of 0.5 to 2.5 kV, a value of  $\sim 1$  kV having been presently used.

5. Coincidence Unit:

UC 676 A with a resolving time adjustable between 0.1-2  $\mu$  sec. on one of the input channels.

6. Timer:

ET 454 A

7. Scalars:

DS 327 A

For counting pill-box samples, a sample changer, with provision for holding four samples and counting these in turn under identical geometrical conditions, was used with the two scintillation detectors mounted vertically above and below  $\sim 5$  cm apart. A 10 cm thick lead shield around each counter head provided adequate background reduction.

For counting a loaded grinding wheel, the sample-changer disc was unscrewed from its axle and replaced by a special aluminium plate. The grinding wheel, after being wrapped in a polythene bag (to minimise any chances of contamination of the counters) was enclosed in a flat perspex box which could be screwed into a fixed position at one end of the aluminium plate. A repeatable counting geometry was thus ensured, with the wheel centre located along the axes of the counter heads.

Plate 3 gives a general view of the counting set-up and also shows the arrangement used for grinding-wheel counting.

#### 4.5 Activation of Steel Workpieces:

The workpiece material used was annealed H.S.S. containing  $\sim 0.1\%$  Cobalt (BHN of  $\sim 240$ ). The main  $\gamma$ -emitting radiotracers to be generated were Fe-59 and Co-60.

The service irradiation of three workpieces (pre-ground to the required size), together with accurately-weighted reference samples of workpiece material, was carried out in the CIRUS reactor by the Isotope Division, BARC. The conditions requested for the irradiation were a thermal flux of  $\sim 10^{12}$  n/cm<sup>2</sup> sec. and a duration of 2-3 hours, the expected activities in  $\mu$  Ci/gm being  $\sim 1$  of Fe-59 and  $\sim 0.2$  of Co-60 [12].

After receipt of the irradiated material at IIT Kanpur,  $\gamma$ -spectra of the samples were observed using NaI and Ge(Li) detector systems, coupled to a 128-channel analyser. Fig.4.2 compares the NaI  $\gamma$ -spectrum with that of a standard Co-60 source. The Ge(Li) spectrum of the irradiated samples is shown in Fig. 4.2(a). A Ge(Li) spectrum of the samples taken  $\sim 4$  months later is shown in Fig. 4.2(b). Comparison of the two Ge(Li) spectra shows that the Fe-59 activity decayed by a factor of  $\sim 1/8$  during this period, relative to the Co-60 activity ( $T_{\frac{1}{2}} = 45$  days for Fe-59, compared to 5.2 years for Co-60). Such decay during the total period of experimentation did not have to be explicitly considered



since a reference sample of workpiece material was used in every experiment for normalising the count-rates.

The three different workpiece samples (Nos. S-3491, S-3495, and S-3496) were counted using a NaI dector with the counting channel set to cover the Fe-59 and Co-60 photopeaks. Their relative activities were obtained by taking 200-second counts with a fixed sample-to-detector distance. Table 4.1 summarises the results.

Table 4.1: Inter-calibration of the Three Different Workpiece Samples.

Sample No.	Mass (grams)	Background corrected counts	Relative specific activity	Sp. activity relative to S-3496
S-3491	0.1921	76.1	$396 \pm 3$	1.256
S-3495	0.1829	54.8	$299 \pm 2$	0.950
S-3496	0.2950	93.0	$315 \pm 2$	1.000

It is seen that there is significant variation between the three specific activities, due probably to finite differences in the irradiation positions used in CIRUS for the three workpiece/sample sets. In the present work, it was the workpiece corresponding to S-3496 that was used throughout. Sample S-3496 itself was cut into four small pieces which were accurately weighed and used as reference pieces for the counting.

#### 4.6 Activation of Aluminium Samples:

A material of particular interest for carrying out loading studies is aluminium, since it is very ductile and difficult to grind due to the ease with which it loads. Although most of the present work was with annealed HSS, a loading experiment with activated aluminium was also carried out to establish the feasibility of generating suitable radiotracers for materials of interest other than steels.

Since  $(n, \gamma)$  activation of aluminium (100 % Al-27) is very difficult to apply to radiotracer experiments ( $T_{1/2}$  is only 2.3 min. for Al-28), it was felt that Na-24 ( $T_{1/2} = 15$  hours, 1.37 and 2.75 MeV coincident  $\gamma$ 's) should be used as the tracer. This could be generated by employing the Al-27  $(n, \alpha)$  reaction with fast neutrons. The cross-section for this reaction is shown in Fig. 4.4 [16].

Initially, the activation of aluminium pieces was attempted by using a 5 Ci Pu-Be source. Such a source has a yield of  $\sim 10^6$  n/cm-sec with an average neutron energy of  $\sim 4$  MeV [17]. Since the fraction of neutrons above the Al<sup>27</sup>  $(n, \alpha)$  threshold ( $\sim 6$  MeV) was small and since the available flux was  $< 10^5$  n/cm<sup>2</sup>-sec, the Na-24 activity obtained was too low for carrying out loading experiments. The characteristic- $\gamma$  spectrum of Na-24, however, was clearly observable from the irradiated workpiece itself.

Activation using the Institute's 2 MeV Van de Graff generator as a source of 14 MeV neutrons proved quite satisfactory for the work. The  $\text{Al}^{27} (n, \alpha)$  cross-section peaks at  $\sim 13$  MeV (Fig. 4.4) so that 14 MeV neutrons obtainable from the  $\text{H}^3 (d, n) \text{He}^4$  reaction are highly suitable for the activation. A 8 Ci tritium target obtained from B.A.R.C. was used with a bombarding deuteron energy of  $\sim 0.9$  MeV. The aluminium pieces were mounted  $\sim 6$  cm, from the target, and a deuteron current of 60  $\mu\text{A}$  was employed giving a total 14 MeV neutron yield of  $\sim 10^9 \text{ sec}^{-1}$  [18]. The aluminium pieces were irradiated for  $\sim 48$  hours, so that the Na-24 activity was close to saturation. This activity was found to be quite adequate for carrying out loading experiments using the extrapolation method for normalization (i.e. employing singles counting only).

Fig. 4.5 shows the  $\gamma$ -spectrum of the activated aluminium pieces. The decay of activity for one of the samples was followed for a period of  $\sim 3$  days. A plot of the count-rate Vs. time, was obtained on a log-linear scale and yielded a half-life of  $(14.6 \pm 0.5)$  hrs. (confirming that the activity was almost completely due to Na-24). In order to check whether the aluminium pieces (of size  $\sim 25 \text{ mm} \times 15 \text{ mm} \times 12 \text{ mm}$ ) had been activated uniformly, one of them was sliced into a number of small pieces by cutting in three perpendicular

directions and the relative specific activity of each small piece was determined. It was found that there was no measurable heterogeneity of the activity in the plane normal to the incident neutrons.

It should be mentioned that the relatively short half-life of Na-24 is a considerable advantage in the sense that there is no danger of any long-term contamination of the grinding machine and working area. However, the 15-hour half-life does mean that the grinding experiments have to be carried out soon after the generation of the activity (i.e. within a day or two). This is quite feasible when a 14 MeV neutron generator, as at IIT Kanpur, is readily available.

#### 4.7 Radiological Considerations:

General radiological protection aspects were outlined in Sec. 2.4. Based on these considerations, the present experiments were carried out in an isolated room. Since the specific activity of the workpieces was not very high, handling and monitoring of the workpiece could be carried out using 30 cm. long, surgical tongs. Lead shielding for the workpiece, when in position on the grinding machine, was found unnecessary as adequate distances could be maintained during the experiment for the received dose to be well within 50 mR per test. An air-contamination monitor and an area monitor were used at all stages of experimentation with the

activated workpiece. A regular film-badge service was utilized for maintaining a record of the dose received during the course of the entire work.

The floor in the working area was covered with rubber sheeting to minimise the spread of any loose activity, while transferring the debris-collection box and the grinding wheel to the work table, etc. An apron, over-shoes and hand gloves were used throughout. The danger of chip activity becoming airborne during the grinding and dressing operations was minimised through the use of the debris-collection box as discussed in Sec. 4.3. As a further precaution, a mask was worn during these machining operations.

For counting purposes, the grinding wheel was wrapped in polythene. The dressed-debris samples were scraped into double-walled pill-boxes, all such sample preparation being carried out in a separate aluminium tray placed on the work table. The tray was monitored periodically and cleaned carefully if any contamination was detected.

## CHAPTER V

### EXPERIMENTS, RESULTS AND THEIR INTERPRETATION

This chapter deals with the various experiments carried out to study characteristics of the loading phenomenon in grinding. Loading curves were obtained for different grinding conditions for the annealed HSS work material. The techniques discussed in Chapter III for obtaining absolute results were compared in four of the experiments. The repeatability of the measurements was tested by employing the same grinding conditions for three of the experiments and comparing the results. A few conventional measurements were also carried out using the method outlined in Sec. 3.3.2.

Finally, an interpretation of the loading data obtained for the different experiments has been attempted.

#### 5.1 Procedure for Obtaining Relative Loading Curves:

Experiments were performed under dry, plunge grinding conditions. The wheel and workpiece specifications are given in Table 5.1.

Table 5.1: Wheel and Workpiece Specifications.

Wheel used	38A46J8VBE (Grindwell-Norton) 127 mm x 16 mm x 32 mm
Wheel speed	3000 r.p.m.
Work material	Annealed HSS, S-3496, BHN ~ 240
Size of workpiece	20.0 mm x 10.06 mm x 10 mm

Prior to each experiment, the grinding wheel (after removal of loaded material from the previous experiment) was counted for any residual activity on its faces (Sec. 3.3.1). This count-rate was taken as wheel background, to be subtracted from each reading. The wheel was then dressed and trued by means of a diamond dresser. In order to obtain consistent results, a fixed dressing sequence was employed at this stage (Table 5.2).

Table 5.2: Dressing Sequence Employed.

---

(i)	Two passes with diamond dresser, infeed of 0.026 mm per pass.
(ii)	Two passes with diamond dresser, infeed of 0.013 mm per pass.
(iii)	Two passes with diamond dresser, infeed of 0.000 mm per pass.
Wheel speed during dressing	: 3000 rpm
Average linear speed of diamond dresser during each pass	: 0.02 m/min.

---

To obtain the first point on the loading curve, the grinding operation was carried out with the activated work-piece for typically 10 passes. The wheel was then removed from the spindle and singles counted on the NaI counting set-up for 200 secs. The sum of the two singles count-rates obtained, after appropriate background subtraction, was taken as the relative measure of the loaded amount of work material.

The wheel was then mounted back into position on the grinding machine. In order to obtain repeatable mounting conditions, the front face of the spindle casing, the rear and front flanges, as well as the faces of the grinding wheel, were suitably marked.

The grinding operation was then continued with the partially loaded wheel for another 10 passes, after which the wheel was removed from the machine and counted once again to yield a second point on the loading curve (corresponding to a total of, now, 20 passes). In this manner, points on the loading curve could be generated for (say) 30, 40, 60, 80, 100, 120 passes. It should be mentioned that a reference piece of the work material was counted periodically during the experiment to take into account any drift in the electronics. Further, the room background was also periodically checked. The statistical error for each point on the relative loading curves obtained was typically  $\pm 4$  percent.

The abscissa used for the loading curves was volume of material removed,  $V_r$ , as measured by a CM-10 dial gauge (Sec. 4.1).

The measurement of normal ( $F_n$ ) and tangential ( $F_t$ ) forces was attempted simultaneously during all the experiments. However, initially, it was not possible to get proper recorder output due to extraneous pick-up. This fault was eliminated during the latter experiments, after making suitable ground connections.



## 5.2 The Various Experiments with Annealed HSS:

A number of experiments were performed with the activated annealed HSS workpiece under different grinding conditions, by varying depth of cut ( $d$ ) and table speed ( $v$ ) (Table 5.3).

Table 5.3: Grinding Conditions for the Various Experiments with Annealed HSS.

Experiment No.	1	2,3,4	5	6	7	8	9	10
Depth of cut, $d$ (mm)	0.013	0.0065	0.0195	0.0065	0.0065	0.0065	0.00975	0.00975
Table speed, $v$ (m/min.)	5.0	5.0	5.0	3.66	2.7	6.0	6.0	5.0

The loading curves obtained for the various experiments are shown in Figs. 5.1 to 5.8.

In all the experiments, the nature of the loading curve was found to be similar (Figs. 5.1 - 5.8). Thus, a newly dressed wheel was seen to load rapidly during the initial stage of grinding (Stage I). The loading then seemed to approach an equilibrium, steady-state value. Thus, during this second phase (Stage II), the loading remained nearly constant or increased only at a very slow rate.

A simple interpretation of the above would be that initially (Stage I), there is rapid filling of the free (empty)

pores on the wheel's cutting surface. Stage II represents a region of dynamic equilibrium in which the amount of freshly loaded material is equal to the amount of loaded material removed due to wheel wear.

In Experiments 1,2,3,4 (Figs. 5.1, 5.2), it was observed that after Stage II, the loading increased and approached a slightly higher 'plateau'. This increase in loading was found to be due to the appearance of small burrs on the sides of the workpiece. With the plunge grinding conditions employed, this meant that some fresh (new) cutting surface of the wheel was exposed to these burrs and that this would start loading rapidly. Other measurements (Sec. 5.7) indicated that, although the burrs had appeared, the wheel was still cutting efficiently at this point.

### 5.3 Normalisation to Absolute Results:

The relative loading curves only indicate the nature of loading. However, if results obtained in different experiments, with possibly different work materials (Sec. 5.8), are to be compared, the amount or volume of loaded material must be obtained.

This was done by using the normalization techniques described in Chapter III. Thus, the amount of loaded material at the end of an experiment was determined via  $\gamma$ - $\gamma$  coincidence counting of the wheel and a reference piece of work-material

(Sec. 3.1). A correction of  $(-3 \pm 2)$  percent was applied in deducing results from Equation (5), Sec. 3.1, to account for angular correlation effects. This correction was obtained by coincidence counting a standard Co-60 source placed first at the centre of the wheel and then at the wheel circumference, the difference in the absolute activity results obtained representing the effects of angular correlation for the wheel counting geometry.

The mass of loaded material at the end of the experiment, deduced in this way, viz.  $M_{lf}$ , was converted to volume using the measured density of the work material ( $8.6 \text{ gm/cm}^3$ ). With the end point of the loading curve thus normalised, the entire curve was rendered absolute in terms of  $V_l$  (loaded volume) - vs -  $V_r$  (volume removed).

Normalisation via  $\gamma$ - $\gamma$  coincidence counting of the wheel was carried out explicitly only in Experiments 1,2,3 and 4, in view of the relatively long counting times required for obtaining adequate coincidence statistics for the wheel (typically  $\pm 3$  percent after 12 hours of counting). The second normalisation technique, i.e. the extrapolation method (Sec.3.2), was, however, applied in all the ten experiments. Fig.5.9 gives a typical curve obtained for the extrapolation method and indicates that the extrapolation correction for the singles counting of the reference pieces on the wheel periphery (Sec.3.2) was only  $\sim 2$  percent.

In order to confirm the validity of the above two techniques, the loaded material was collected during dressing at the end of Experiments 1,2,3 and 4 and was counted in coincidence in pill-box geometry. To the absolute amount of loaded material thus obtained, a correction was applied for the residual activity on the wheel's faces (Sec. 3.3.1), thus yielding the total amount that had been loaded on the wheel.

#### 5.4 Comparison of Normalisation Techniques:

Absolute results obtained by using the three different normalisation techniques are compared in Table 5.4. It is seen that the results obtained, viz.  $V_I$ ,  $V_2$ , and  $V_3$ , agree with each other within the indicated statistical errors of typically  $\pm 4$  percent. This shows that the presently developed techniques yield consistent results for the loaded volume  $V_1$ .

The last column in Table 5.4 gives the value of loaded volume for Experiments 2,3 and 4, as deduced from singles counting of the wheel using the absolute results from coincidence counting during Expt. 1. The consistency here shows that absolute results once obtained for a particular experiment (either by coincidence counting of the wheel or the extrapolation method) can be used to normalise the relative singles count-rates in other experiments. This is provided the geometry offered by the wheel (i.e. the diameter of the wheel) does not vary much between the experiments, and further that a

Table 5.4: Comparison of Normalisation Techniques.

Expt. No.	Loaded volume from wheel coincidence counting $V_I(\text{mm}^3)$	Loaded volume from extrapolation method $V_2(\text{mm}^3)$	Volume of material in dressed debris $V_d(\text{mm}^3)$	Volume of material remaining on wheel after dressing $V_x(\text{mm}^3)$	Loaded volume from dressed sing $(V_d + V_x) = V_3(\text{mm}^3)$	Loaded volume calculated from wheel singles counts using coincidence results from Expt. No. 1
1	$2.36 \pm 0.09$	$2.66 \pm 0.06$	$1.93 \pm 0.05$	$0.58 \pm 0.05$	$2.51 \pm 0.07$	$2.36 \pm 0.09$
2	$1.15 \pm 0.06$	$1.18 \pm 0.05$	$0.98 \pm 0.03$	$0.16 \pm 0.01$	$1.14 \pm 0.03$	$1.13 \pm 0.06$
3	$1.50 \pm 0.05$	$1.64 \pm 0.06$	$1.54 \pm 0.04$	$0.09 \pm 0.01$	$1.63 \pm 0.04$	$1.46 \pm 0.08$
4	$1.47 \pm 0.05$	$1.54 \pm 0.06$	$1.43 \pm 0.04$	$0.20 \pm 0.02$	$1.63 \pm 0.05$	$1.37 \pm 0.08$

reference piece is counted simultaneously during the experiments to take into account any decay of activity as well as drifts in the counting system.

### 5.5 Comparison Between Radiotracer and Conventional Measurements:

A few conventional measurements were carried out with unirradiated work material for the grinding conditions of Expts. 2,3 and 4 using the technique discussed in Sec. 3.3.2. Results thus obtained are compared in Table 5.5 with those obtained by the radiotracer method.

Table 5.5: Comparison of Conventional and Radiotracer Measurements.

No. of Passes	Volume of Material Loaded ( $\text{mm}^3$ )				
	Conventional				Radiotracer
	Mass of grains plus loaded material (gm)	Mass of grains (gm)	Mass of loaded material (gm)	Corrected loaded volume ( $\text{mm}^3$ )	Loaded volume ( $\text{mm}^3$ )
5	1.16487	1.16190	0.00297	0.38	0.34
10	1.36253	1.35761	0.00492	0.63	0.56
15	1.67155	1.66401	0.00754	0.96	0.73
20	0.84383	0.83593	0.00795	1.01	0.87
30	2.90470	2.89600	0.00870	1.11	1.01

It is seen that the results obtained from the conventional measurements are typically 10 percent greater than those

from the radiotracer techniques. The agreement is still very encouraging, considering (a) the sources of error in the conventional method used (e.g., the deduction of loaded mass from the difference of two nearly equal weights (Table 5.5)), and (b) the fact that the repeatability of loading experiments (Sec. 5.6) is only  $\sim 10$  percent.

#### 5.6 Repeatability of Results:

Three experiments, viz. Experiments 2, 3 and 4, were carried out under identical grinding conditions ( $v = 5.0$  m/min,  $d = 0.0065$  mm), to check the repeatability of results. The loading curves for the three experiments are compared in Fig. 5.2. It is seen that results are repeatable to only  $\sim \pm 10$  percent due to the randomness of various mechanisms in the grinding process.

#### 5.7 Interpretation of Loading Data:

From the plots of forces ( $F_n$  and  $F_t$ ) shown in Figs. 5.6, 5.7, and 5.8, (for Expts. 8, 9, 10 respectively), it is seen that Stage II of the loading curves lies in a region of stable forces. It is thus indicated that the 'equilibrium' loaded amount (Sec. 5.2) was established during the time the grinding process was taking place in an efficient manner. This was further confirmed by the fact that the volume removal rate was constant throughout these experiments (Fig. 5.10).

The 'steady-state' loaded volume is what would effect certain important variables in the grinding process, e.g. surface finish, power consumption, etc. From this point of view, it was felt that a parameter to characterise Stage II of the loading curve should be studied for its variation with grinding conditions. The loaded volume corresponding to  $V_r = 55 \text{ mm}^3$  was chosen as this parameter, since it was found that, in each of the present experiments, the loaded volume  $V_{155}$  (corresponding to a volume removal of  $55 \text{ mm}^3$ ) lay on the 'plateau' of the loading curve.

Fig. 5.11 shows the variation of  $V_{155}$  with depth of cut  $d$  ( $v = 5.0 \text{ m/min.}$ ) and table speed  $v$  ( $d = 0.0065 \text{ mm}$ ). The errors indicated on the experimental points include  $\pm 10$  percent due to the repeatability constraint (Sec. 5.6). It is seen that  $V_{155}$  increases with  $d$  in the manner indicated. However, the variation with  $v$  is not that clear. This is probably due to the limited range of table speeds presently investigated. Higher  $v$ -values could not be achieved with the present set-up without causing significant vibration of the table.

From an empirical point of view, it was felt that a parameter characterising the loading phenomenon should depend on some appropriate combination of the cutting conditions, such as volume removal rate ( $vd$ ), or chip thickness



( $\propto v^{1/2} \cdot d^{1/4}$ , Sec. 2.1.2). Fig. 5.12 and 5.13 show the variation of  $V_{155}$  with  $vd$  and  $v^{1/2} d^{1/4}$  for all the different experiments conducted. (The effect of the variation in wheel diameter -  $\sim 10$  percent between Experiments 1 and 10 - has been presently neglected in considering the chip thickness). Although smooth curves have been drawn through the experimental points in both Figs. 5.12 and 5.13, it should be noted that a particular parameter cannot, by definition, be expected to vary smoothly with both  $vd$  and  $v^{1/2} d^{1/4}$ . In order to establish if  $V_{155}$  indeed varies with one of these, and if so, which one, it would be necessary to carry out a much larger number of experiments covering a wider range of grinding conditions (particularly for  $v$ ) than presently investigated.

Although Stage II of the loading curve was presently deemed important, it has not been established that the nature of the loading curve would be similar for other wheel/work combinations. It is possible that in other situations, Stage I may be a more significant region. This may be characterized in several possible ways, e.g. by the  $V_r$ -value which gives a loaded volume equal to half the 'equilibrium' value. The method presently adopted was to assume that the approach to equilibrium could be expressed by the following relation between  $V_l$  and  $V_r$ .

$$V_{155} - V_1 = \exp(-a V_r)$$

where 'a' is a constant, characterizing the rate at which the loaded volume approaches  $V_{155}$ . By plotting  $(V_{155} - V_1)$  against  $V_r$  on a log-liner scale, straight lines were indeed obtained for the 'elbow' region of the loading curves, the slopes of these lines giving appropriate values for the different experiments.

Fig. 5.14 shows the variation of 'a' with  $d$  and  $v$ . Fig. 5.15 and 5.16 show the variation with  $vd$  and  $v^{1/2} d^{1/4}$ . It is seen that the experimental point for Expt. 10 does not seem consistent with the other data. This could be due to some systematic error in this particular experiment. However, It should be mentioned that the value of 'a' was found to be strongly dependent on the exact manner in which the loading curve was fitted to the very few experimental points available in the 'elbow' region. Thus, to some extent, the results obtained for  $a$  were rather ambiguous.

## 5.8 Loading Measurements with Aluminium:

As mentioned in Sec. 4.6, activation of aluminium was achieved using the Van de Graff generator at IIT Kanpur as a 14 MeV neutron source. A loading experiment was carried out with the activated sample of aluminium, using the same wheel as earlier and the following grinding conditions:

Wheel speed : 2000 rpm  
Depth of cut : 0.0065 mm  
Table speed : 5.0 m/min  
Workpiece size : 25.0 mm x 15.4 mm x 11.5 mm

The experiment was carried out as explained in Sec. 5.1, except that appropriate decay corrections had to be applied to each reading ( $T_{\frac{1}{2}}$  for Na-24 = 15 hours) for obtaining the relative loading curve. The results were normalised by employing the extrapolation method. Fig. 5.17 shows the normalised loading curve obtained.

It is seen that the loaded volume on the wheel surface increases rapidly to a very much higher value than in the annealed HSS experiments (even after accounting for the larger width of the aluminium workpiece). This can be explained partly by the differences in material properties and partly by the fact that the wheel wear would be greatly reduced in the aluminium experiment. The latter would imply a very much smaller removal rate for the loaded material and hence an approach to 'saturation' (with the material filling the pores completely) rather than an approach to a state of dynamic equilibrium for the loaded material (Sec. 5.2). It is such excessive loading which effects the grindability of aluminium.

## CHAPTER VI

### CONCLUSIONS AND SCOPE FOR FURTHER WORK

#### 6.1 Conclusions:

The loading phenomenon in grinding is difficult to study experimentally by conventional means. Although a few systematic investigations of the phenomenon have been tried out earlier, some of the methods that were employed are rather painstaking, while others provide difficulties in obtaining absolute results.

Radiotracer techniques have been developed and applied for the first time to the evaluation of the loading of grinding wheels. It has been shown that they provide a simple and highly sensitive means for study of the phenomenon.

Various loading experiments were carried out with activated annealed HSS workpieces, Co-60 and Fe-59 being the  $\gamma$ -emitting tracers used. Two techniques were applied for normalising the relative loading curves obtained through singles  $\gamma$ -counting of the wheel's cutting surface, viz.,

- (a)  $\gamma$ - $\gamma$  coincidence counting of the Co-60 activity and
- (b) an extrapolation method for the singles counting. By comparing absolute results obtained using the above two techniques as well as coincidence counting of dressed

debris, consistency between the different radiotracer methods was established within statistical error of typically  $\pm 4$  percent.

A comparison of loaded volumes deduced by the nuclear methods was made with some conventional measurements involving the chemical separation of grains from dressed debris. The agreement obtained was satisfactory, considering the errors in the conventional measurements as well as the repeatability of loading experiments (presently established as about  $\pm 10$  percent).

The normalisation of loading curves by  $\gamma$ - $\gamma$  coincidence counting of the wheel involves relatively long counting times (typically 12 hours) to obtain adequate statistical accuracy. Further, this technique can be used only if the available radiotracer decays by the simultaneous emission of two  $\gamma$ -rays. On the other hand, the extrapolation method can be applied to any available  $\gamma$ -emitting radiotracer with a not-too-short half-life. Also, since only singles  $\gamma$ -counting is involved, adequate statistical accuracy can be achieved in a relatively short period. It has been seen in the present experiments that the extrapolation corrections (to account for the different counting geometry and self-absorption effects for the reference work-material pieces stuck symmetrically on the wheel periphery) <sup>were</sup> ~~were~~ only  $\pm 2$  percent. It must be stressed,

however, that for any applied technique, measurements should be carried out while taking all necessary precautions to minimise systematic errors and eliminate possible ambiguities (e.g., the finite possibility of some work material sticking to the wheel's non-cutting faces during grinding (Sec. 3.3.1)).

Investigation of the loading data presently obtained for annealed HSS was carried out by considering two characteristic stages of the loading curves, viz., (a) Stage- I in which there is a rapid increase of loaded material and (b) Stage - II in which the loaded amount remains nearly constant. The latter was interpreted as a steady-state value representing dynamic equilibrium between further loading and wheel wear. The variation of characteristic loading parameters defined for these two stages was studied with grinding conditions, viz., table speed ( $v$ ) and depth of cut ( $d$ ) as well as appropriate combinations of  $v$  and  $d$ . While a clear dependence of loading on  $d$  was observed, the range of conditions investigated was not wide enough to draw more fundamental conclusions about the loading phenomenon.

A loading experiment was conducted for an activated aluminium workpiece, using Na-24 as the radiotracer. The latter was generated via 14 MeV ( $n, \alpha$ ) activation, using the IIT Kanpur Van de Graaf. Employing the extrapolation method

for normalisation, it was found that the loaded volume for aluminium was very much greater than for the steel. This was interpreted as being partly due to the much smaller wheel-wear rate in the aluminium experiment, so that the loaded material would tend to fill pores on the wheel's cutting surface more completely.

## 6.2 Scope for Further Work:

Presently, only a single wheel/work combination has been studied in some detail. It would be important to investigate whether the nature of the loading curve is similar for other combinations. Thus, it has been demonstrated how radiotracers can be generated and used for studies with steels (Fe-59 or Co-60) and aluminium (Na-24). Brass is an example of another material of interest for loading experiments. Here the tracers that could be used are Zn-65 ( $T_{1/2} = 245$  days) from  $(n, \gamma)$  activation of zinc, or Cu-64 ( $T_{1/2} = 12.8$  hours) from Cu-63  $(n, \gamma)$  or Cu-65  $(n, 2n)$ .

The range of grinding conditions presently considered was rather limited, partly due to inadequacies of the grinding set-up used. A much more comprehensive set of experiments would have to be carried out in order to establish whether an empirical relationship exists between loading and some grinding parameters such as volume removal rate, chip thickness or chip length.

The presently developed methods for loading studies should be applied in parallel with measurements of other basic grinding variables, such as surface finish, grinding ratio (wheel wear) and grinding coefficient (forces), so that a clear understanding of the phenomenon and its effects can be evolved. The optimization of wheel specifications, grinding conditions and the choice of cutting fluid could then be carried out in an appropriate manner. Experiments could be conducted for studying the variation of wheel-life, as defined in terms of some critical volume of loaded material.

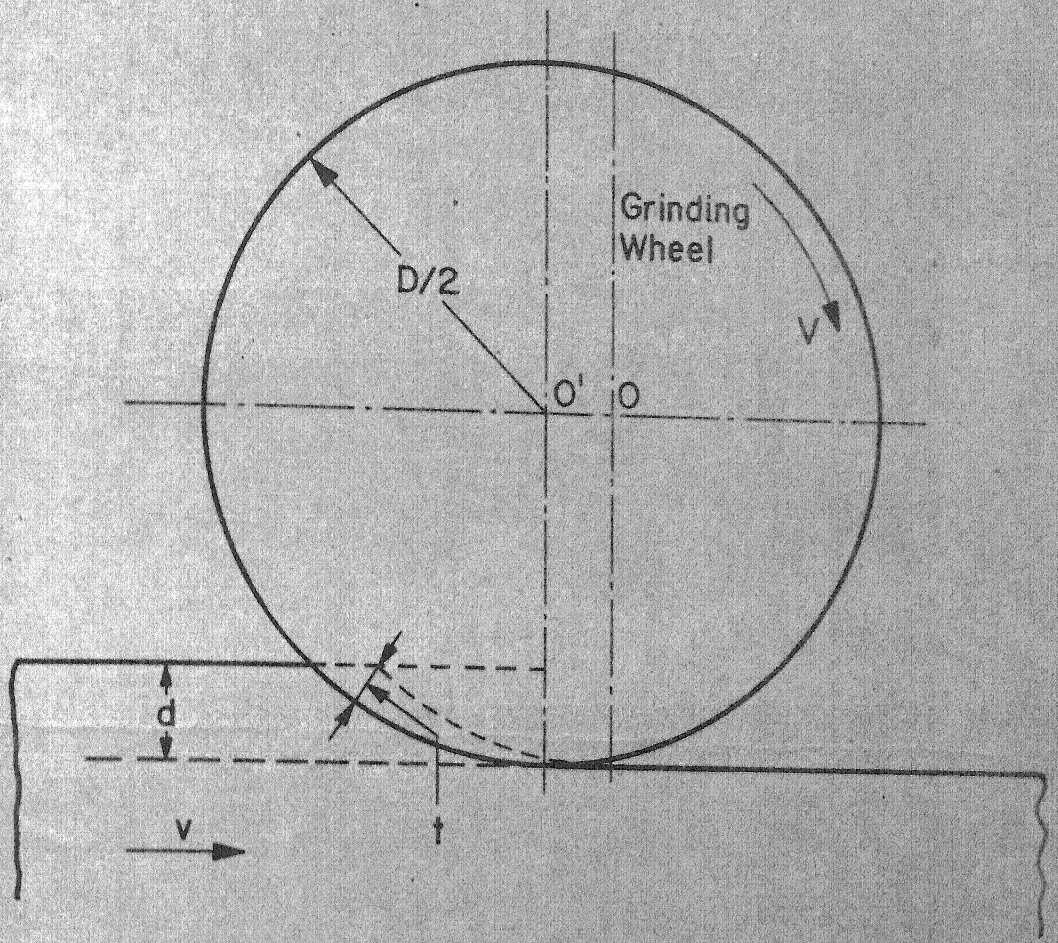
The same basic radiotracer methods as presently applied to grinding could be used for studies of loading in honing, another important finishing process.



## REFERENCES

1. Armarego, E.J.A., and Brown, R.H., 'The Machining of Metals', Prentice Hall, Inc., 1969.
2. Reichenbach, G.S., Mayer, J.E., Kalpakcioglu, S., and Shaw, M.C., 'The Role of Chip-Thickness in Grinding', Trans. ASME (May 1956) 847.
3. Shudolz, L.H., Manilych, S., and Mapes, G.S., 'A Method of Measuring the Metallic Wheel Loading Characteristics', Mechanical Engg., Vol. 72 (1950) 963.
4. Khudobin, V.V., 'Cutting Fluid and its effects on Grinding Wheel Clogging', Machines and Tooling, Vol.XL, No. IX, 548.
5. Pandey, P.C., Ashok Kumar, and Neema, M.L., 'Clogging of Grinding Wheels', Fifth AIMTDR Conference (April 1972) 31.
6. Sata, T., Suto, T., Waida, T., and Noguchi, H., 'In-Process Measurement of the Grinding Process and Its Applications', New Developments in Grinding, Carnegie Press, 1972.
7. Yamamoto, A., and Maeda, V., 'Magnetic Methods for In-Process Measurement of Abrasive Tools' Loading', Bull. Japan Soc. of Prec. Engg., Vol. 8, No.3 (Sept. 1974).
8. Merchant, M.E., and Krabacher, E.J., 'Radioactive Tracers for Rapid Measurements of Cutting Tool Life', J. of Appl. Physics, 22 (1951) 1507.
9. Colding, B.N., and Erwall, L.G., 'Wear Studies of Irradiated Carbide Cutting Tools', Nucleonics, Vol.11, No. 2 (1953) 46.
10. Wilson, G.F., and McHenry, W.D., 'Study of the Radiometric Method and Use of the Liquid Scintillation Technique for Tool Wear Determination', Trans. ASME, J. of Engg. for Ind., 87 (1965) 47.

11. Cook, N.H., and Lang, A.B., 'Criticism of Radioactive Tool Life Testing', Trans. ASME, J. of Engg. for Ind., 85 (1963) 381.
12. Bhattacharya, S.L., 'Absolute Tool-Wear and Tool-Life Determination Via  $\gamma$ - $\gamma$  Counting of Radiotracers', M.Tech. Thesis, I.I.T. Kanpur, 1976.
13. Siegbahn, K., Ed., ' $\alpha$ ,  $\beta$ ,  $\gamma$ -Spectroscopy, Vol. 1', North Holland, 1965.
14. Pandey, S.J., 'Wheel Wear In Dry Surface Grinding', M.Tech. Thesis, I.I.T., Kanpur, 1974.
15. Shaw, M.C., 'Metal Cutting Principles', 3rd Ed., MIT, Cambridge Press, 1954.
16. Stehn, J.R., et al., 'Neutron Cross Sections', BNL-325, Second Edition, Supplement No. 2, Vol. 1, 1965.
17. Krishnamony, S., and Raghunath, V.M., 'Handbook of Health Physics Data', Report No. BARC/I-55, 1969.
18. Bygrove, W., Treado, P., and Lambert, J., 'Accelerator Nuclear Physics', High Voltage Engg. Corporation, USA, 1970.



$v$  = Table Speed  
 $d$  = Depth Of Cut (Down Feed)  
 $V$  = Wheel Speed  
 $t$  = Chip Thickness  
 $D$  = Wheel Diameter

Fig.2.1 Variables In Surface Grinding



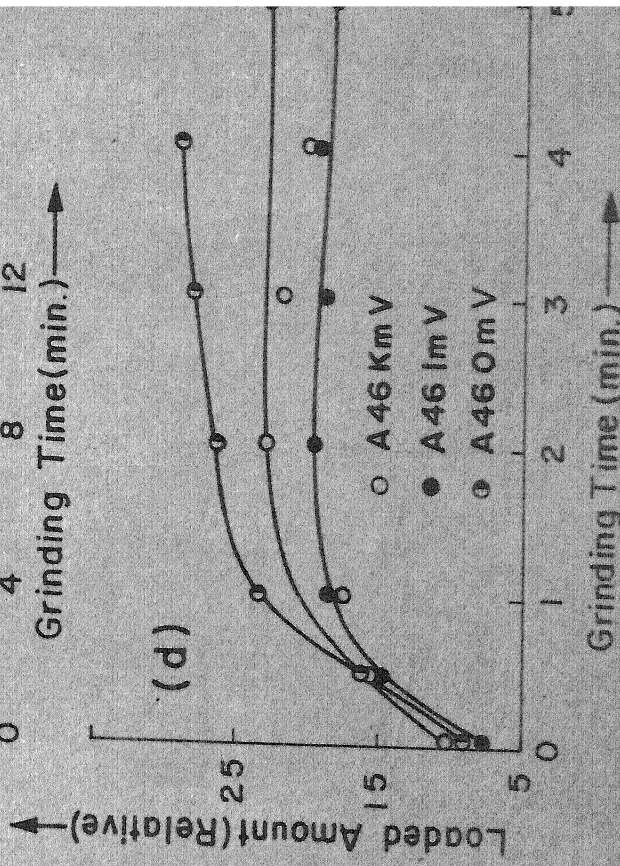
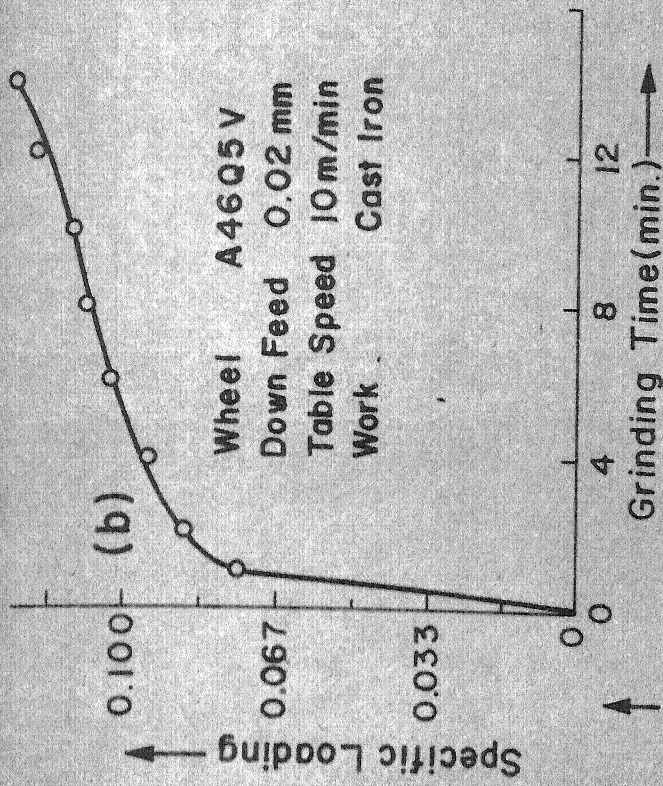
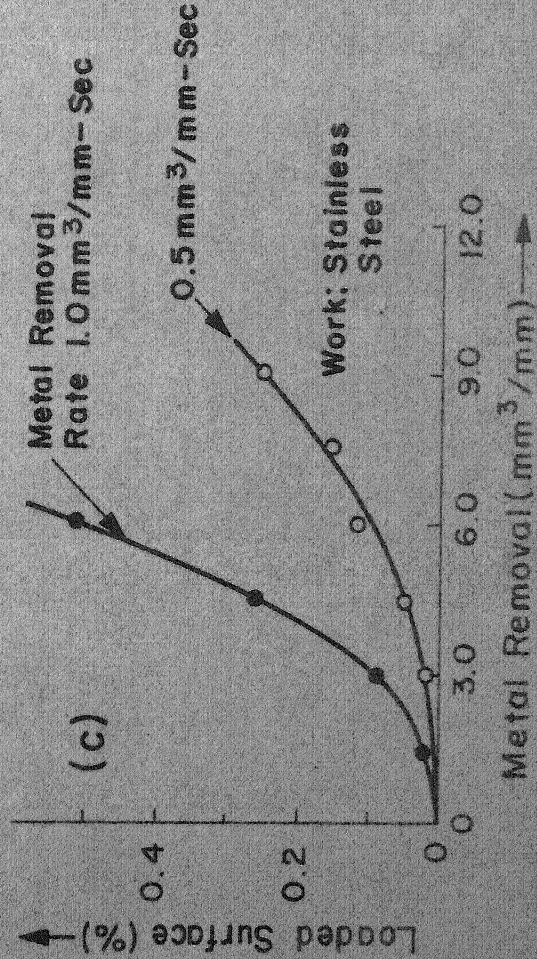
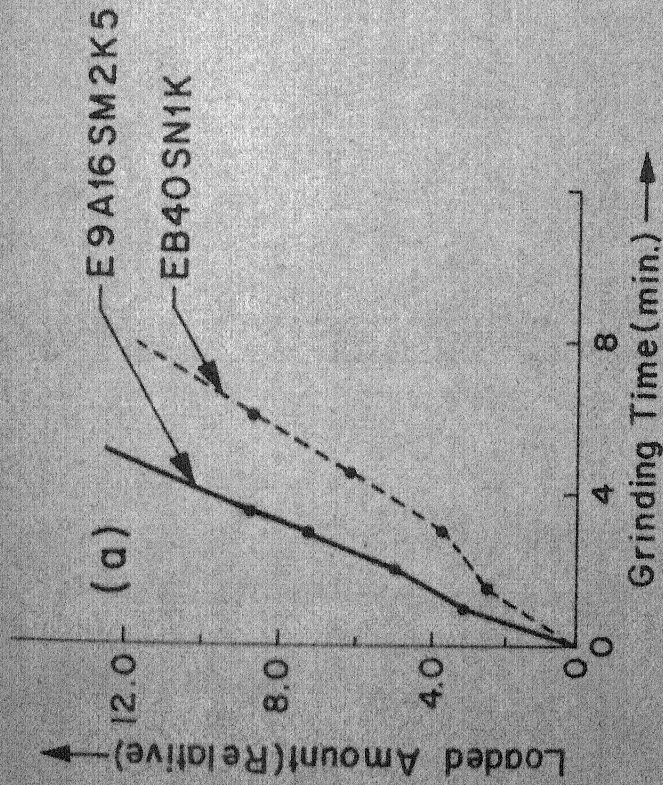


Fig.2.2 Loading Curves From Reference No.(a)4,(b)5,(c)6,(d)7

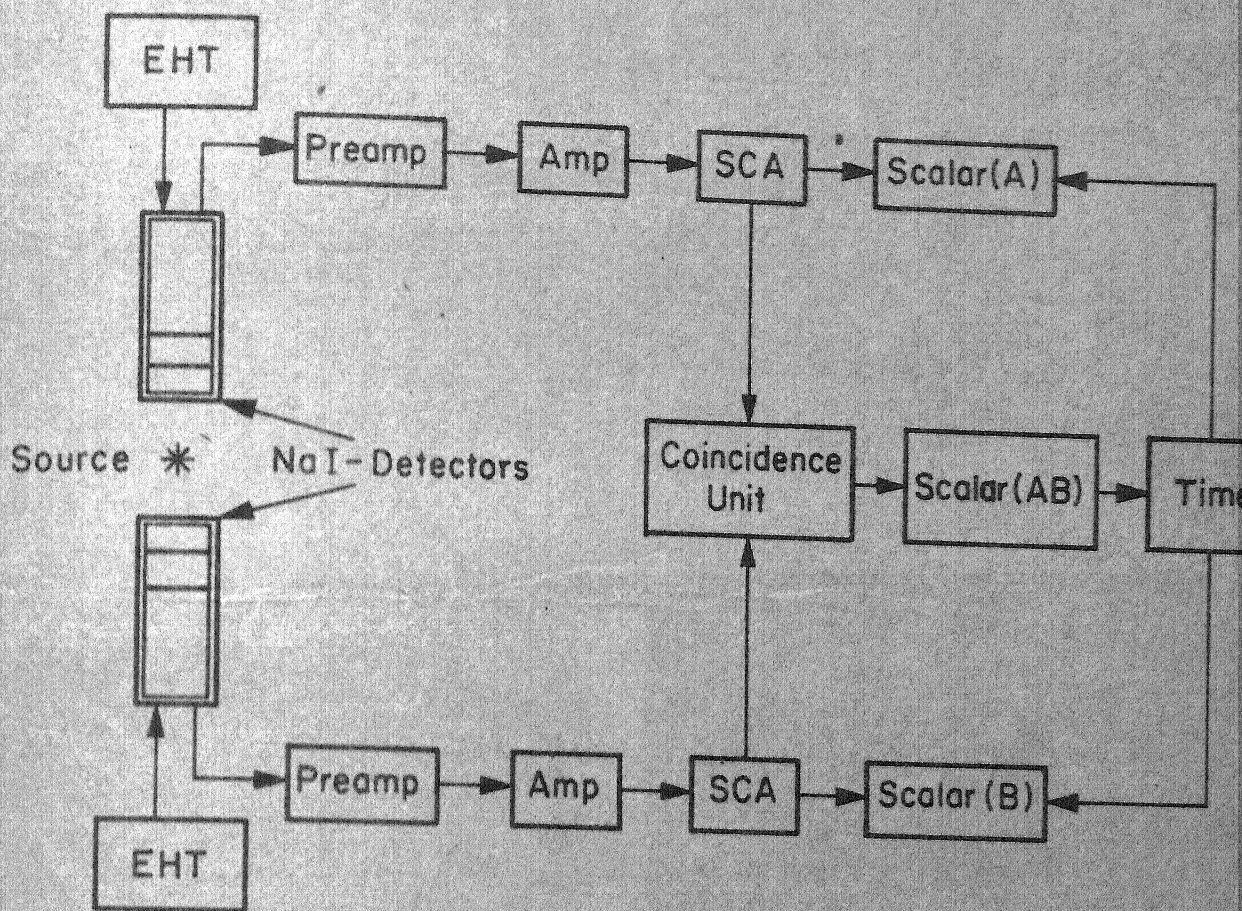


Fig.3.1 Block Diagram Of  $\gamma$ - $\gamma$  Coincidence Counting Setup.



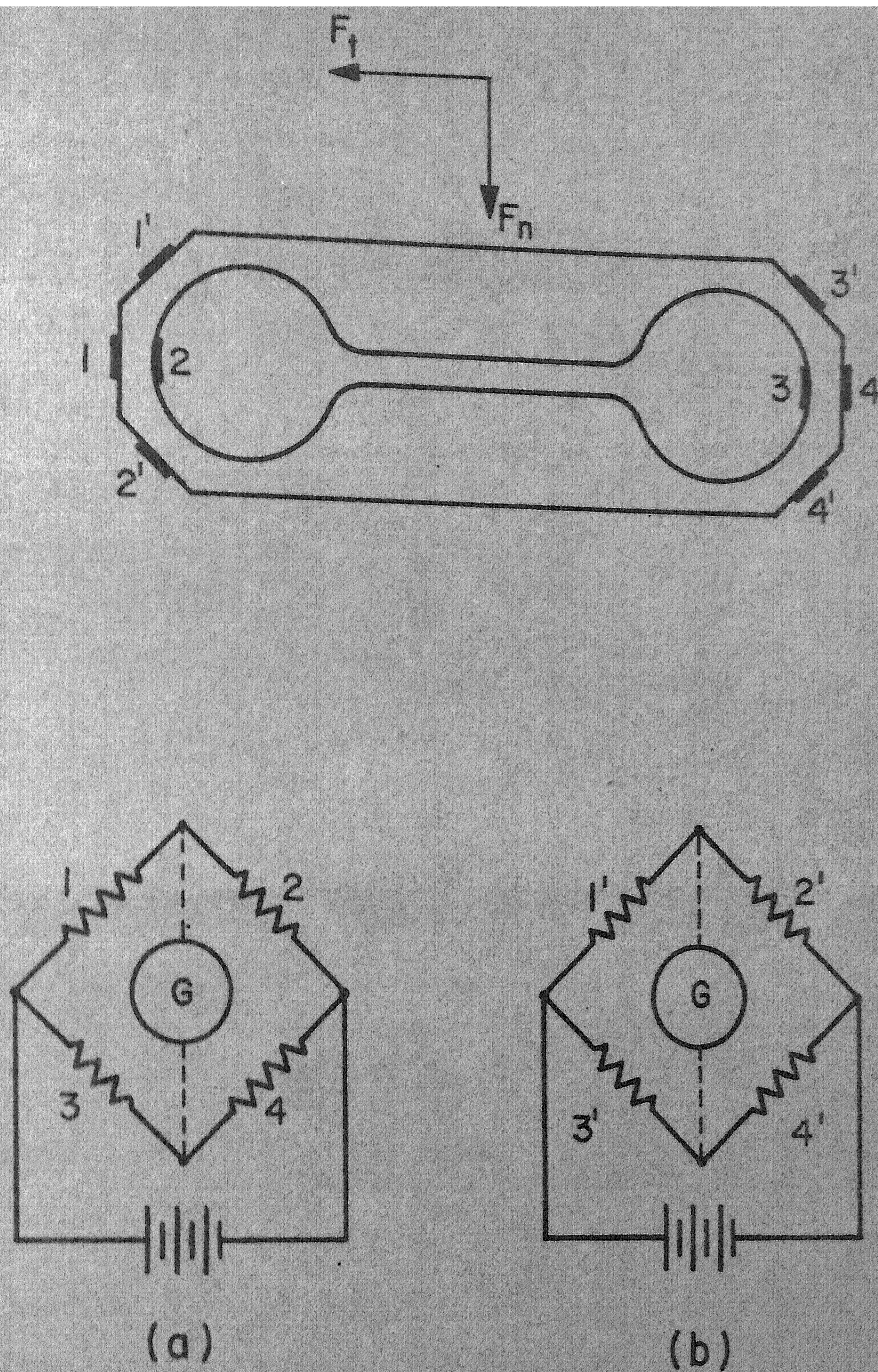
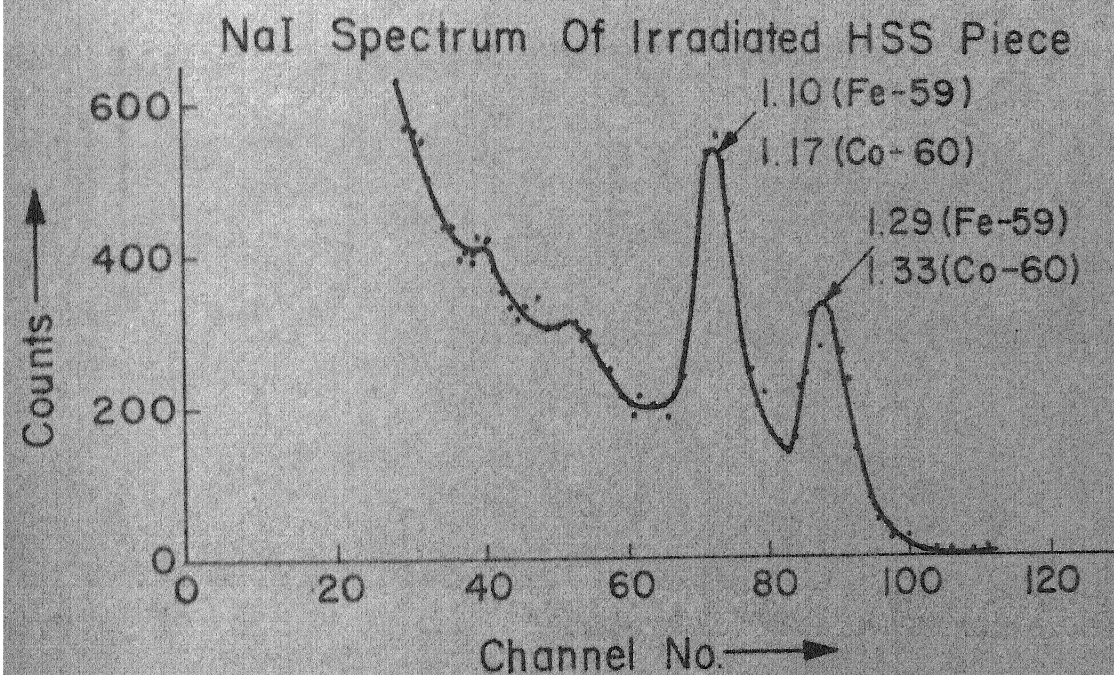
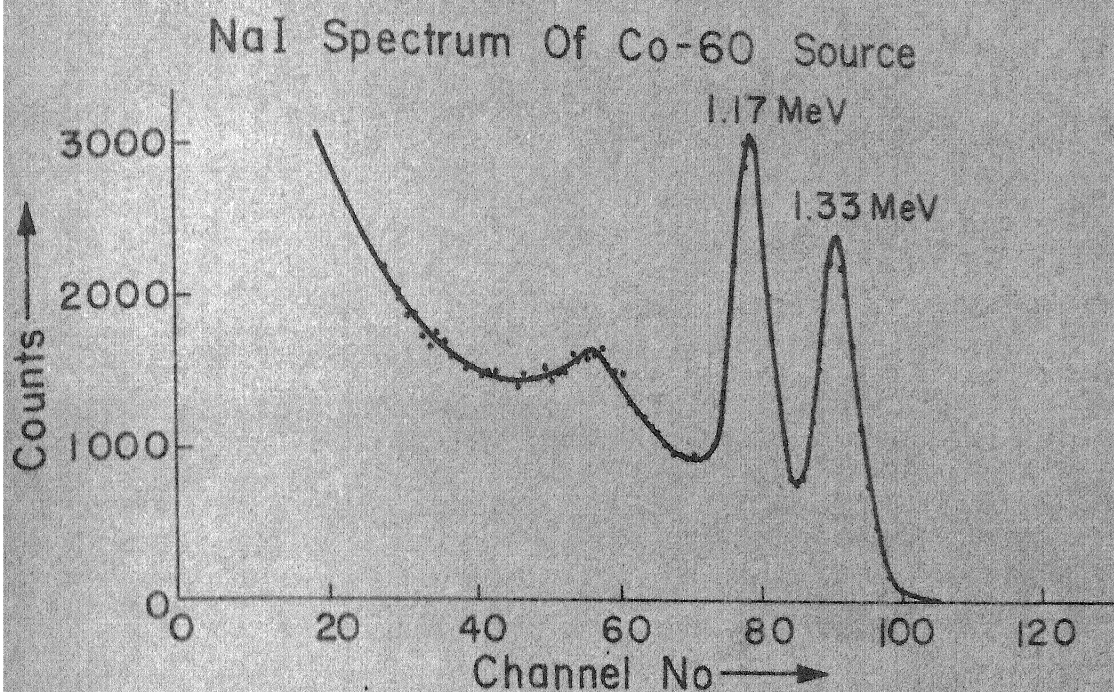


Fig. 4.1 Extended Octagonal Ring Type Dynamometer  
 (a) Wiring Diagram For Vertical Force  
 (b) Wiring Diagram For Horizontal Force



g.4.2 Comparison Of NaI Spectra Of Standard Co-60 Source And Irradiated Annealed HSS Piece.



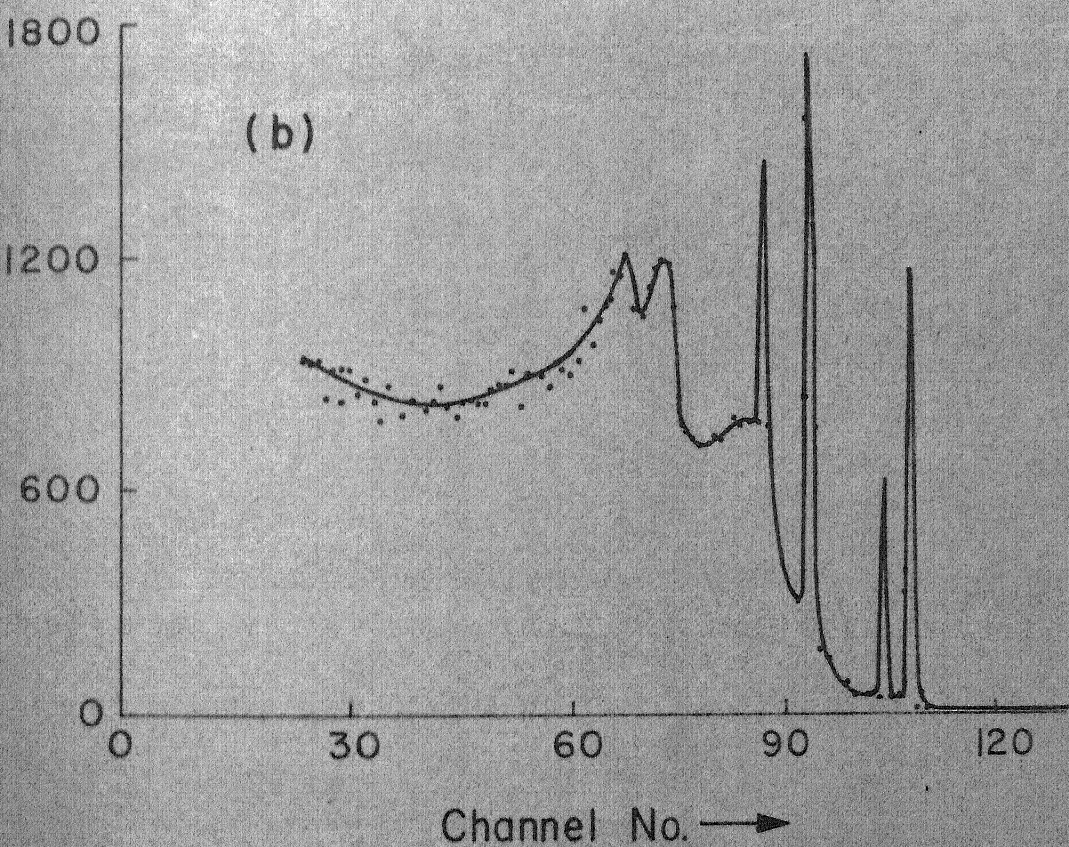
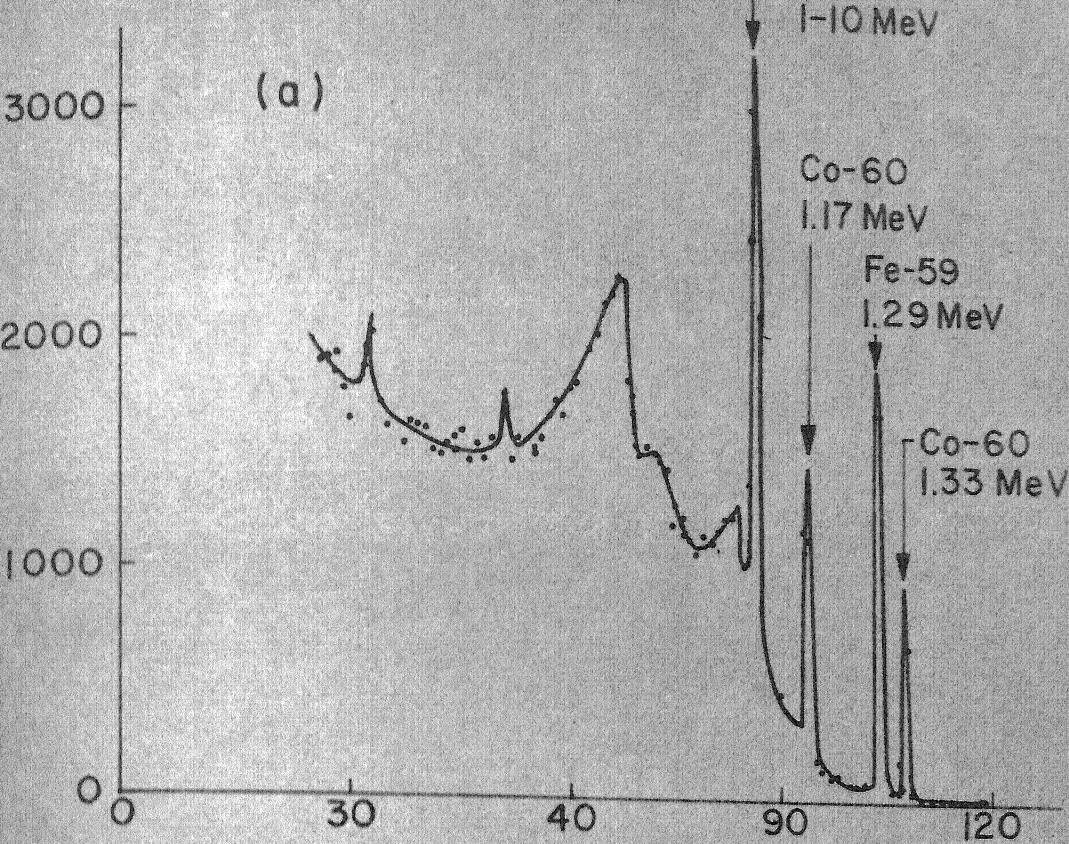


Fig. 4.3 Ge (Li) Spectra Of Irradiated Steel Samples  
(a) 2 Weeks, (b)  $4\frac{1}{2}$  Months After Irradiation



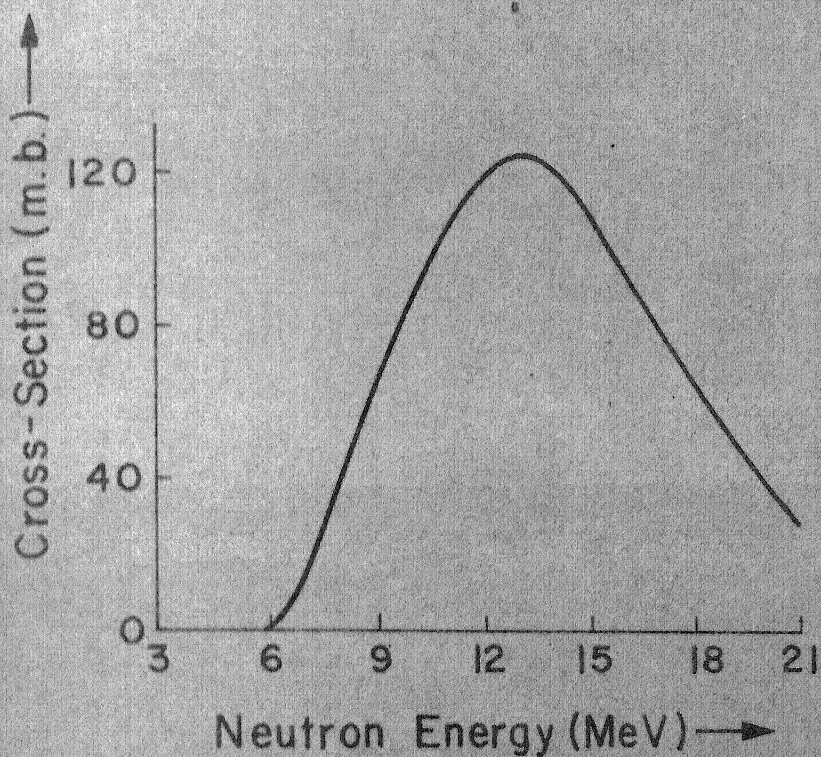


Fig.4.4 Neutron Cross-section For  $\text{Al}^{27}(\text{n}, \alpha)\text{Na}^{24}$  Reaction [Ref. No.16]